The role of MDM2-NBS1 protein interaction in DNA repair in bladder cancer

A thesis submitted for the degree of Master of Science by Research

By

Kristina Aare

St Edmund Hall

CRUK/MRC Oxford Institute for Radiation Oncology

Department of Oncology

University of Oxford

Supervisor

Professor Anne Kiltie

Word count: 18,784

CANCER RESEARCH UK | MRC Medical Research Council

OXFORD INSTITUTE FOR RADIATION ONCOLOGY

UNIVERSITY OF OXFORD

Acknowledgements

I would like to thank my supervisor, Professor Anne Kiltie, and Dr Judith Nicholson for the patient guidance, encouragement and advice they have provided during this project. My sincere thanks also go to Dr Eva McGrowder and Dr Samantha Knight for their help and advice during the CNV project. Professor Ester Hammond, I have appreciated your practical assistance, thoughtful feedback and moral support every step of the way. Finally, to all the friends and colleagues who have shaped my days and continue to do so, I salute and thank you.

Contents

List of figures

List of tables

List of abbreviations

AA Amino Acid

AD Acidic Domain

ATM Ataxia-Telangiectasia Mutated

BCG Bacillus Calmette-Guérin

BD Binding Domain

BRCA1 Breast Cancer Type 1 susceptibility protein

BRCT1/2 BRCA1 C-Terminus domain

BS Binding Site

CIS Carcinoma *In Situ*

CNA Copy Number Abnormality or Alteration

CNV Copy Number Variation

DDR DNA Damage Response

DMEM Dulbecco's Modified Eagle Medium

DMSO Dimethyl Sulfoxide

DSB Double Strand Break

ER Estrogen Receptor

FBS Foetal Bovine Serum

FHA Forkhead-Associated Domain

gDNA Genomic DNA

Gy Gray

HR Homologous Recombination

IB Immunoblotting

IF Immunofluorescence

IP Immunoprecipitation

IR Ionising Radiation

KSFM Keratinocyte Serum-Free Medium

Leu Leucine

MDM2 Mouse Double Minute 2

MEM Minimum Essential Media

MIBC Muscle-Invasive Bladder Cancer

MMEJ Microhomology-Mediated End Joining

MRN MRE11-RAD50-NBS1

mRNA Messenger RNA

MVAC Methotrexate – Vinblastine – Doxorubicin (Adriamycin) – Cisplatin

NBN Nibrin

NBS Nijmegen Breakage Syndrome

NES Nuclear Export Signal

NLS Nuclear Localisation Signal

NMIBC Non-Muscle Invasive Bladder Cancer

PBS Phosphate Buffered Saline

PCR Polymerase Chain Reaction

Phe Phenylalanine

PTM Post-translational Modification

RING Really Interesting New Gene finger domain

RPMI Roswell Park Memorial Institute medium

SNP Single Nucleotide Polymorphism

Trp Tryptophan

WCL Whole Cell Lysate

ZNF Zinc Finger domain

Abstract

The role of MDM2-NBS1 protein interaction in DNA repair in bladder cancer

A thesis submitted for the degree of Master of Science by Research by Kristina Aare

St Edmund Hall, University of Oxford

Trinity 2017

MDM2 is an E3 ubiquitin ligase that is frequently amplified in human cancers, including muscle-invasive bladder cancer. While it has a firmly established role in negative regulation of the tumour suppressor p53 by proteasomal degradation, the p53-independent functions of MDM2 remain scarcely understood. One of them is the delay of DNA double-strand break repair via a direct binding interaction with NBS1 of the MRE11-RAD50-NBS1 DNA repair complex.

RG7388 is a selective MDM2 inhibitor, a second-generation member of the nutlin family that is currently in early clinical trials for solid and haematological tumours. The inhibition of MDM2-p53 protein interaction by RG7388 has no radiosensitising effect and does not disrupt the MDM2-NBS1 protein interaction in T24 and RT112 cells. However, compared to untreated controls, RG7388 alone and in combination with 5 Gy of ionising radiation (IR) alters the mRNA levels of MDM2 and NBS1 and protein levels of MDM2. NBS1 and MDM2 do not form any foci but co-localise in the nuclei of T24 and RT112 cells four hours after exposure to IR.

In this study, we show that MDM2-NBS1 is an important protein interaction that remains intact in unstressed T24 and RT112 cells and following their exposure to genotoxic ionising radiation alone or in combination with RG7388. Under the same treatment conditions as well as in untreated controls, the pilot western blot experiment suggests that NBS1 is not ubiquitylated

either in T24 or RT112 cells. Further experiments are required to verify this finding and to detect and characterise other post-translational modifications that may be involved in regulation of the MDM2-NBS1 protein interaction to determine its impact on DDR.

Chapter 1 Introduction

1.1 The hallmarks of cancer

Cancer is a generic term for a group of malignant neoplastic diseases characterised by uncontrolled cell division. The hallmarks of cancer comprise ten biological characteristics that govern the multi-step malignant transformation of normal cells (Figure 1.1). Genome instability is an underlying universal characteristic that contributes to the genetic diversity of cancers. The emerging hallmarks include inflammation, reprogramming of energy metabolism and evading immune surveillance (Hanahan and Weinberg, 2000, 2011).

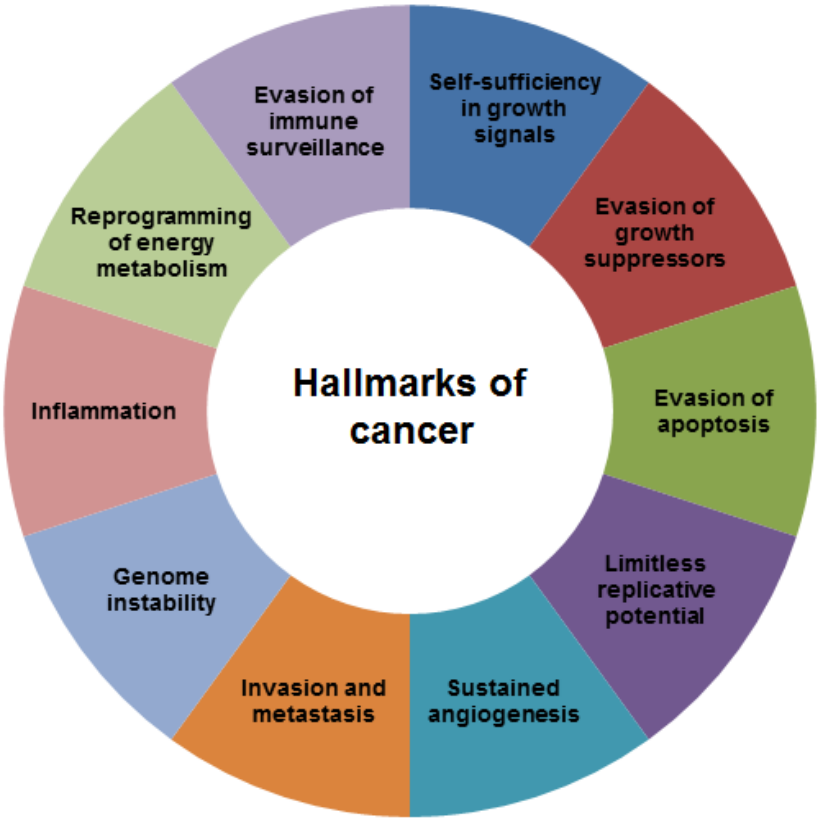

Figure 1.1: The hallmarks of cancer (adapted from Hanahan and Weinberg, 2011).

1.2 Bladder cancer

Bladder cancer arises from the epithelial lining (i.e. the urothelium) of the urinary bladder (Van Batavia *et al.,* 2014). It is the ninth most common cause of cancer death in Europe (Antoni *et al.,* 2017). Approximately 70% of all newly diagnosed bladder cancer cases are non-muscle invasive

(NMIBC), including stage Ta, T1 and carcinoma *in situ* (CIS) (Nepple and O'Donnell, 2009). With optimal treatment, there is a 90% 5-year survival rate for non-muscle invasive bladder cancer (NMIBC) and 40-60% for organ-confined muscle-invasive disease (MIBC) (T2-3) (Figure 1.2). However, disease recurrence continues to pose a significant clinical challenge (Cancer Research UK).

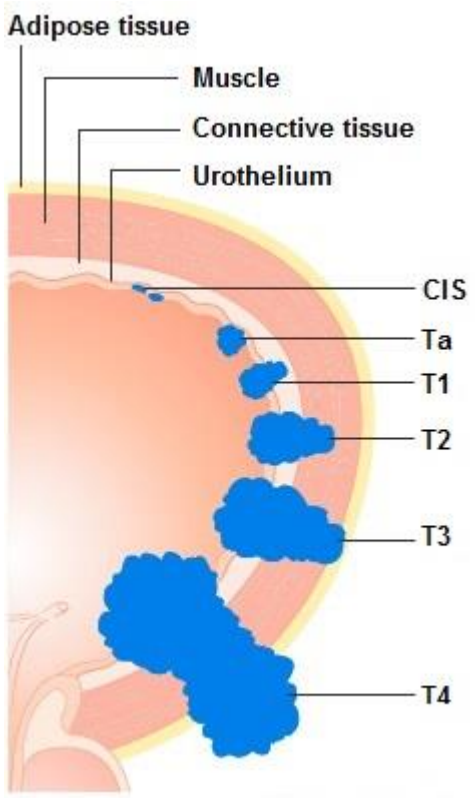

Figure 1.2: Bladder cancer tumour (T) stages (adapted from Cancer Research UK).

For non-muscle-invasive bladder cancer, the standard treatment is complete resection of the tumour followed by intravenous chemotherapy or, in more high-risk cases, Bacillus Calmette-Guérin (BCG) immunotherapy (Kawai *et al.*, 2013). For muscle-invasive bladder cancer, the treatment regimen involves neoadjuvant chemotherapy followed by radical cystectomy or bladder-preserving treatment with chemoradiation (El-Taji *et al.,* 2016). Patients with advanced bladder cancer are treated with systemic cisplatin-based chemotherapy, or immunotherapy if first-line chemotherapy cannot control the disease (Farina *et al.,* 2017). Recent genomic analyses

refined the classification of molecular subtypes of bladder cancer and identified novel opportunities for therapeutic development (Knowles and Hurst, 2015; Kamat *et al.*, 2016).

1.3 Molecular subtypes of muscle-invasive bladder cancer

The molecular and histological heterogeneity of muscle-invasive bladder cancers accounts for the high variability in clinical outcomes in response to conventional chemotherapy. To date, there are three main molecular subtypes identified for MIBC according to the MD Anderson Cancer Center (Figure 1.3 A-B) (Choi *et al.*, 2015). They are similar to the already established molecular subtypes of breast cancer (Perou *et al.*, 2000). Basal MIBCs are characterized by p63 activation (Karni-Schmidt *et al.*, 2011; Choi *et al.*, 2014), squamous differentiation (Figure 1.3A) (Sjödahl *et al.*, 2012; Choi *et al.*, 2014), and more aggressive disease at presentation (Kim *et al.*, 2012; Mitra *et al.*, 2014). Luminal MIBCs can be distinguished by active PPARγ (Ayers *et al.*, 2007), oestrogen receptor (ER) and its co-activator Trim-24 transcription enrichment (Tsai *et al.*, 2010), with activating FGFR3 mutations and potentially FGFR inhibitor sensitivity (Figure 1.3B) (Choi *et al.*, 2014). The p53-like subtype involves a subset of luminal and basal tumours with upregulation of p53 and p53-pathway-related genes. Other overexpressed protein biomarkers of the p53-like tumours include Caveolin-1, Collagen VI, Fibronectin, and PKC alpha (Choi *et al*., 2014, Dadhania *et al.,* 2016). p53-like MIBCs are consistently resistant to neoadjuvant Methotrexate – Vinblastine – Doxorubicin (Adriamycin) – Cisplatin (MVAC) chemotherapy (Choi *et al.*, 2014).

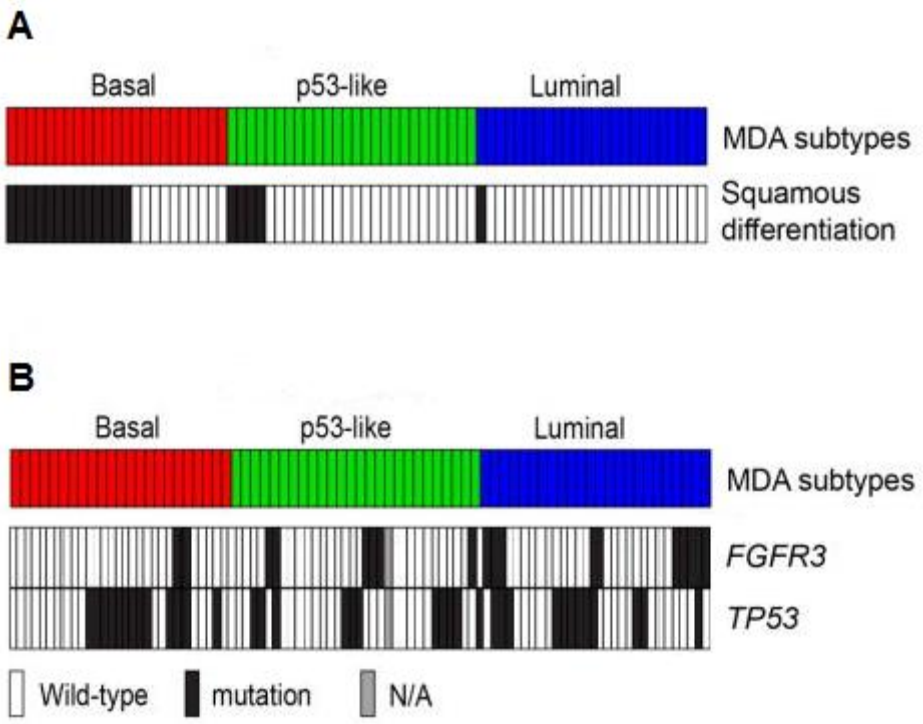

Figure 1.3: Relationship between the MD Anderson subtypes **(A)** and squamous feature content, and **(B)** FGFR3 and TP53 mutations (adapted from Choi *et al.*, 2014)

1.4 Structure and function of MDM2 protein

The preservation and maintenance of genomic stability provide a biological barrier against cancer initiation. Therefore, studies on the mechanism of action of genomic instability mediators hold significant clinical value (Yao and Dai, 2014). Mouse double minute 2 (MDM2) is a thoroughly studied regulator of the p53 tumour suppressor and an oncogene (Bouska *et al.*, 2008; Kato *et al.*, 2017).

MDM2 is frequently overexpressed in human and murine malignancies, including MIBC and cases that have inactivated the tumour suppressor p53 (Wang *et al.*, 2008; Lushnikova *et al.*, 2016). Increased expression of Mdm2 in murine B lymphocytes inhibits p53 and p21 expression, reduces B cell susceptibility to p53-dependent apoptosis, increases the frequency of chromosomal aberrations and facilitates lymphomagenesis (Lushnikova *et al.*, 2016).

MDM2 is a 489 aa E3 ubiquitin ligase, an interaction hub for more than 100 proteins and transducer of different signalling pathways (Nicholson *et al.*, 2012; Fåhraeus and Olivares-Illana, 2014). It is upregulated in response to p53-activating genotoxic stimuli, such as γ-irradiation, hyperproliferative signals and hypoxia (Levine *et al.,* 2006). As an E3 ligase, MDM2 regulates the protein levels of p53 by tagging it with K48-linked ubiquitin chains recognised by 26S proteasome leading to subsequent proteasomal degradation (Honda *et al.,* 1997). By binding to p53 at its N-terminal transactivation domain, MDM2 can also directly block the transcription activation function of p53 (Momand *et al.,* 1992; Ma *et al.,* 2006). In addition to negative regulation of p53 (Meek, 2015), MDM2 also functions as a molecular chaperone (Wawrzynow *et al*., 2007), regulator of ribosomal biogenesis (Deisenroth and Zhang, 2010) and mRNA translation (Candeias *et al.,* 2008).

The key to this functional and interactional diversity of MDM2 is its structural and regulatory complexity. The N-terminal section of MDM2 is the lid domain that folds over and regulates association of p53 with the hydrophobic pocket (aa 18–101). The central region of MDM2 protein domain structure contains the NBS1 binding site (aa 198-314), the nuclear localisation (NLS; aa 179–185) and nuclear export signals (NES; aa 190–202) that allow for this protein's translocation between the nucleus and cytoplasm. The C-terminal RING domain (aa 436–482) promotes E3 ubiquitin ligase activity, harbours nucleotide binding activity, and encompasses the nucleolar localisation signal (464-471 aa) (Alt *et al.*, 2005; Fåhraeus and Olivares-Illana, 2014) (Figure 1.4).

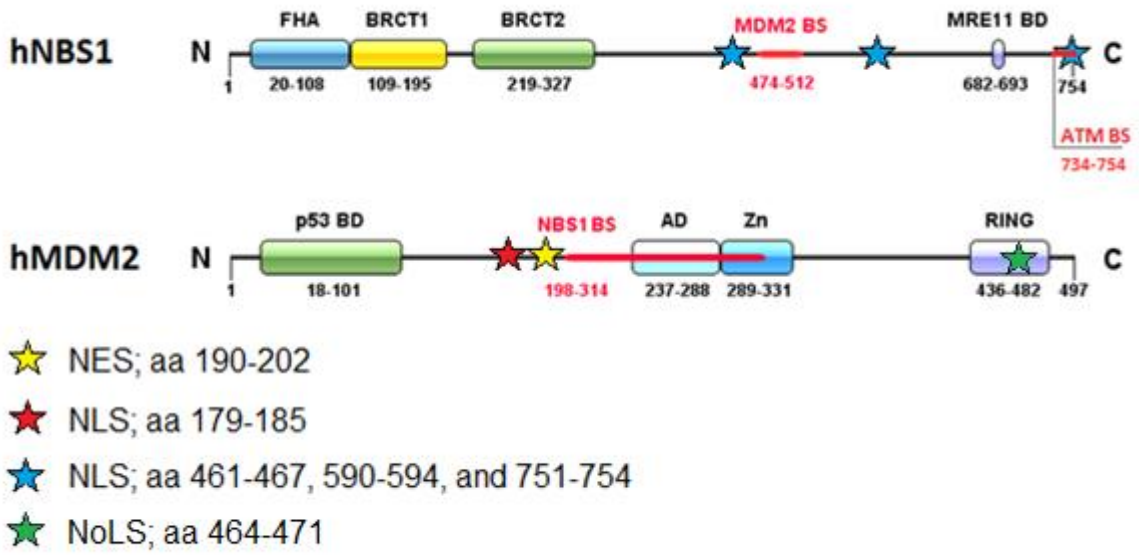

Figure 1.4: Domain structure of human NBS1 and MDM2 proteins: FHA (forkhead-associated domain), BRCT1/2 (BRCA1 C-terminus domain), BD (binding domain), BS (binding site), AD (acidic domain), Zn (zinc finger domain), RING (RING finger domain). MDM2-, NBS1- and ATM binding sites are marked in red. The figure was generated using the Illustrator for Biological Sequences (IBS) (Ren *et al.*, 2009).

1.5 Relationship between MDM2 and MDMX in regulation of p53

The regulation of p53 activity is achieved primarily by ubiquitylation that affects its cellular localisation and turnover. Monoubiquitylation of p53 leads to its nuclear export to the cytoplasm, whereas polyubiquitylation initiates its proteasomal degradation (Kruse and Gu, 2009). Alterations of p53 nuclear concentration or activity affect its ability to interact with chromatin and act as a transcription factor. This modulation of p53 activity is particularly critical during embryogenesis (Itahana *et al.,* 2007), stress response and tumorigenesis (Perry, 2009).

Negative regulation of p53 involves multiple proteins, including RING E3 ubiquitin ligase MDM2 and MDM4, also known as MDMX, a RING-domain protein deficient of E3 ubiquitin ligase activity. There is a hypothesis suggesting that both MDM2 and MDMX emerged as central regulators of p53 as a result of duplication event that occurred at the MDM locus. However, while MDM2

obtained the E3 ubiquitin ligase activity, MDMX became a regulator of MDM2 stability by heterodimerising with it and preventing its auto-ubiquitylation (Momand *et al.,* 2011).

MDM2 and MDMX have a 31% homology at amino acid level and form a dynamic protein-protein interaction by heterodimerising through their C-terminal RING finger domains (Sharp *et al.,* 1999; Marine *et al.,* 2006). This event stabilises MDM2 and results in increased MDM2-mediated mono-ubiquitination of p53 (Mendoza *et al.,* 2014). Unlike MDM2, MDMX expression is not regulated by p53. MDMX cannot independently ubiquitylate p53 to target it for proteasomal degradation (Shvarts *et al.,* 1996). However, MDM2-MDMX heterodimer is reported to be more efficient in downregulation of p53 compared to MDM2 alone (Marine *et al.,* 2006). MDM2 catalyses monoubiquitylation of p53, which can be followed by polyubiquitylation by other E3 ligases. The latter may target p53 for proteasomal degradation. Unlike MDM2 that is involved in regulation of p53 protein levels, MDMX inhibits p53 by binding to and masking its N-terminal transcriptional activation domain, without causing its degradation (Pei *et al.,* 2012).

MDMX is constitutively expressed in healthy murine tissues (Jackson *et al.,* 1999), and its depletion leads to embryonic lethality, which, similarly to MDM2, can be rescued by crossing with p53 null mice (Parant *et al.,* 2001; Migliorini *et al.,* 2002). A study of a knock-in mouse model with intact p53-binding site but abolished RING-E3-ubiquitin-ligase activity of MDM2 has indicated that the Mdm2-p53 interaction, without Mdm2-mediated p53 ubiquitination, cannot control p53 activity sufficiently to allow early mouse embryonic development. It was also reported that in the absence of interaction with MdmX, the function of MDM2 alone was insufficient for inhibition of p53 activity (Pei *et al.,* 2012). This data is consistent with previous *in vitro* experiments by Itahana *et al.,* 2007.

Notably, copy number gain of MDMX is common for multiple different cancer types, including breast-, bladder- and central nervous system tumours (Toledo *et al.,* 2006; Yu *et al.,* 2014). When MDMX copy number gain coincides with elevated MDMX protein expression, it may trigger the downregulation of tumour suppressor p53 at transcriptional and post-translational levels and therefore facilitate the cancer cell survival (Shadfan *et al.,* 2012). Further research is required to gain a better insight into the mechanism of MDM2-MDMX-driven regulation of p53, the structure and dynamics of the MDM2-MDMX-p53 protein complex, its role in tumorigenesis and potential application of its components as tumour biomarkers or therapeutic targets.

1.6 MDM2 and NBS1 in DNA damage repair

There is growing evidence suggesting that in addition to its role as a negative regulator of p53, MDM2 also possesses p53-independent functions, some of which are involved in tumorigenesis (Feeley *et al.,* 2017). For instance, MDM2 overexpression detected in human sarcomas and bladder cancers often co-occurred with p53 mutations or lack of p53 (Bouska *et al.,* 2008; Cordon-Cardo *et al.,* 1994). Patients whose tumours showed both abnormalities had decreased survival rate compared to cases with either abnormality alone (Cordon-Cardo *et al.,* 1994; Lu *et al.,* 2002). The p53-independent oncogenic activity of MDM2 has also been reported in multiple mouse studies (Jones *et al.,* 1998; McDonnell *et al.,* 1999), and its in-depth research is critical for our understanding of the overall contribution of MDM2 to genome instability.

One of the links between MDM2 and genome instability is its protein-protein interaction with NBS1. The NBS1 protein is a product of the mutated *NBN* (nibrin) gene in NBS. Being a component of the MRE11-RAD50-NBS1 (MRN) complex, NBS1 is considered a primary protein to be recruited to DNA double strand breaks (DSBs) as a sensor and mediator of the DNA damage response (DDR) and repair by homologous recombination (HR) and microhomology-mediated end joining (MMEJ)

(Deriano *et al.*, 2010; Lu *et al.*, 2012; Schwertman *et al.,* 2016). NBS1 is also known to regulate chromatin remodelling during DDR by histone H2B ubiquitylation through binding to RNF20 at the C-terminus (Saito and Komatsu, 2015). The C-terminus of NBS1 contains an NLS (aa 751-754) and binding sites for MRE11, a homologous recombination repair nuclease, and ATM (aa 734-754), a key player in signal transduction after the generation of IR-induced DSBs. In humans, a mutation in NBS1 leads to the development of Nijmegen breakage syndrome (NBS), a recessive genetic disorder characterised by increased sensitivity to ionising radiation (IR) and a high frequency of malignancies (Alt *et al.,* 2005; Varon *et al.,* 1998).

The central domains of NBS1 and MDM2 contain binding sites for each other (Alt *et al.*, 2005) (Figure 1.4). MDM2-triggered inhibition of DNA double-strand break repair relies on the NBS1-binding domain of MDM2 and is independent of p53 expression or mutation status (Alt *et al.*, 2005; Conradt *et al.*, 2013; Tonsing-Carter *et al.*, 2015). Interestingly, the C-terminal ubiquitin ligase domain of MDM2 was reported as dispensable for NBS1 binding and DDR downregulation (Alt *et al.*, 2005). This also applies to FHA and BRCT domains of NBS1 required for its co-localisation with γH2AX at sites of DNA DSB breaks (Desai-Mehta *et al.,* 2001; Kobayashi *et al.*, 2002).

Following DNA damage, the MRN complex promotes phosphorylation of ataxia-telangiectasia mutated (ATM), a kinase responsible for DNA damage signaling (Lee *et al.,* 2005; Uziel *et al.,* 2003). ATM then phosphorylates histone H2AX, which is critical for the long-term retention of repair proteins at sites of DNA breaks (Shiloh *et al.,* 2006) (Figure 1.5). As a result of DNA damage response, ATM, MRN complex and other proteins involved in DNA repair form nuclear foci at sites of DNA breaks, which resolve when the DNA damage is repaired. Although the exact mechanism remains to be elucidated, it appears that MDM2 may interfere with NBS1 function in

early DNA damage signalling events. The study by Bouska *et al.,* 2009 indicates that elevated protein levels of MDM2 can delay the phosphorylation of H2AX, ATM signalling and nuclear foci formation and therefore the overall DNA repair (Bouska *et al.,* 2009).

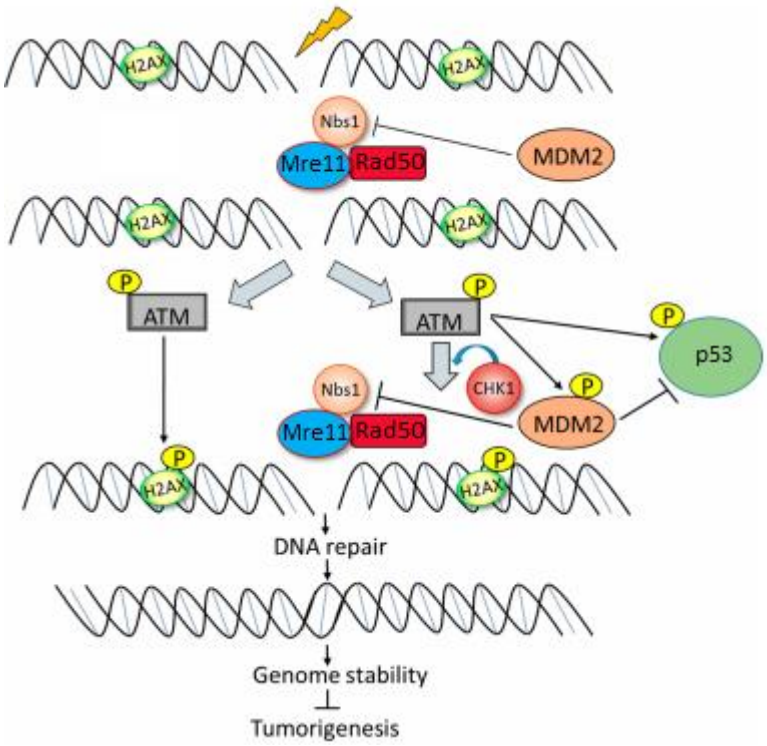

Figure 1.5: Schematic representation of MDM2-NBS1 protein interaction during repair of IR-induced DSBs. Adapted from Saadatzadeh *et al.,* 2017.

Our understanding of the physiological role of delaying the DDR via MDM2-NBS1 interaction remains rather scant. In their studies of MRE11 as a predictive marker for radiotherapy response in MIBC, Choudhury *et al.,* 2010 hypothesised that low expression of MRN complex would allow for better outcome following radical radiotherapy in bladder cancer patients due to reduced efficiency of DNA repair.

The instability of MRN complex indeed lead to failure of induction of the DNA damage signalling. However, it also caused radioresistance due to inefficient activation of the downstream apoptotic cascade and lack of checkpoint arrest forcing continuous cell proliferation. Cells containing an MRE11 frameshift mutation were found to have an impaired S-phase checkpoint (Giannini *et al.,*

2002), and siRNA-mediated knockdown of NBS1 in B-lymphoblasts caused impaired checkpoint activation, reduced apoptosis and radioresistance (Zhang *et al.,* 2000). High expression of MRN complex proteins, by contrast, is associated with improved prognosis and better outcome following adjuvant radiotherapy in bladder- and breast cancer patients (Soderlund *et al.,* 2007, Choudhury *et al.,* 2010). In addition, adenoviral vector-based over-expression of NBS1 was shown to cause radiosensitisation in a head and neck squamous cell carcinoma cell line (Rhee *et al.,* 2007).

Further research is needed to gain more insight into the underlying mechanisms of MDM2 regulation of NBS1 and MRN complex in the context of DNA damage signalling. In addition, knowing that MDM2 interactions are tightly regulated by post-translational modifications (e.g. ubiquitylation, phosphorylation, SUMOylation) that control its conformation, stability, interactions and function, it would be interesting to further investigate which of them initiate and stabilise the MDM2-NBS1 protein interaction (Shi and Gu, 2012; Bueren-Calabuig and Michel, 2016).

1.7 Copy number alterations of *MDM2* and *NBN*

In addition to alternative splicing, post-translational modifications, conformational changes and cellular localisation, the interaction between NBS1 and MDM2 and their functions could be regulated by copy number variations (CNV) of *NBN* and *MDM2* and genes encoding their binding partner proteins (Desjardins *et al.,* 2009; Rayburn *et al.,* 2005; Varon *et al.,* 2006). CNV is a phenomenon in which sections of the genome are repeated and the number of repeats varies between individuals in the human population. CNV is involved in generating natural variation in the population as well as disease phenotypes. In the context of cancer samples, CNVs are referred to as copy number abnormalities (CNAs) (Freeman *et al.,* 2006.)

MDM2 is reportedly overexpressed in many different cancers, with an overall frequency of gene amplification of 7% (Momand *et al.,* 1998; Zhang *et al.,* 2000). Soft tissue sarcomas have the highest mRNA and protein levels of MDM2 (Momand *et al.,* 1998; Rayburn *et al.,* 2005; Zhang *et al.,* 2000). The MDM2 protein overexpression ranges from 8% of various sarcomas to 68% of angiosarcoma samples and often co-occurs with *MDM2* gene copy number gain (Stefanou *et al.,* 1998; Zietz *et al.,* 1998).

Various types of carcinomas are also reported to have increased expression of the MDM2 protein and increased copy number of its gene. Bladder carcinomas, for example, show positive staining for MDM2 in 12% to 49% of tumours (Ioachim *et al.,* 2000; El-Kenawy *et al.,* 2003; Uchida *et al.,* 2002). Only a few studies investigated *MDM2* gene copy number amplification and its potential link to overexpression of mRNA in bladder cancer. However, there are reports suggesting a positive correlation trend between MDM2 gene copy number gain and elevated MDM2 protein expression in bladder cancer (Simon *et al.,* 2002). Other cancer types showing remarkably increased expression of MDM2 include non-small cell lung cancer, prostate-, and ovarian cancers (Momand *et al.,* 1998; Rayburn *et al.,* 2005; Zhang *et al.,* 2000).

MDM2 is a thoroughly studied oncogene and mediator of genomic instability known to contribute to progression of MIBC (The Cancer Genome Atlas Research Network, 2014; Kato *et al.*, 2017). Recently, it has also been reported that MDM2 may be associated with hyperprogression observed in some patients with advanced cancer of different types (Kato *et al.,* 2017; Kato *et al.,* 2018).

By interacting with its ligand (PD-L1), the programmed cell death protein PD-1 acts as an immune checkpoint and promotes self-tolerance by suppressing the effector T-cell activity. Therefore,

cancer cells overexpressing PD-L1 can evade immune surveillance (Dong *et al.,* 2017). Although therapies targeting PD-1/PD-L1 immune checkpoint by single agent inhibitors show high anti-tumour efficacy including long-term remission, there has been observed a subset of patients, so-called hyperprogressors, whose response to treatment included increased rate of tumour growth and overall clinical deterioration.

Next-generation sequencing analysis of 155 tumour samples identified the copy number gain of MDM2 as a potential genomic biomarker of hyperprogression following the anti-PD-1 /PD-L1 monotherapy compared to pre-treatment (Kato *et al.,* 2017). However, immunotherapy can itself indirectly contribute to MDM2 overexpression. PD-1/PD-L1 inhibitors are known to increase IFN-γ level that activates JAK-STAT pathway leading to elevated expression of interferon regulatory factor 8 (IRF8). IRF8 then binds to MDM2 promoter and induces its expression (Saleh *et al.,* 2017).

The link between MDM2 amplification and cancer hyperprogression remains unclear and requires further investigation. Blockage of PD-1/PD-L1 pathway could stimulate tumour growth or tumorigenesis via alternative signaling pathways or upregulation of alternative immune checkpoints. Further genomic investigation is required in order to verify whether MDM2 can be used as a biomarker for hyper-progression on immunotherapy and whether it offers the possibility of apoptotic pathway-targeted p53-independent cancer therapy (Conradt *et al.*, 2013; Tonsing-Carter *et al.*, 2015). To date, the understanding of the relation between copy number and expression for mammalian genes is very limited. It would be interesting to examine how the copy number gain may affect MDM2's expression, interactions and functional impact on DDR in bladder cancer.

1.8 Mechanism of MDM2 inhibition by RG7388

Restoration of p53 activity by inhibition of the p53-MDM2 interaction has been considered an attractive approach for cancer treatment (Bouska *et al.*, 2008; Conradt *et al.*, 2013; Ding *et al.*, 2013; Cazier *et al.*, 2014; Tonsing-Carter *et al.*, 2015). However, the hydrophobic protein-protein interacting surface of the p53-binding pocket in MDM2 represents a significant challenge for the *de novo* synthesis of small-molecule inhibitors with desirable pharmacological characteristics (Ding *et al.*, 2013).

The crystal structure of the N-terminal domain of MDM2 bound to a 15-residue transactivation domain peptide of p53 revealed amino acid residues critical for the MDM2-p53 protein interaction: Phe19, Trp23, and Leu26 (Kussie *et al.*, 1996). RG7388 is a member of the *cis*-imidazoline compound family, termed nutlins, designed to mimic the transactivation domain peptide of p53 and therefore competitively inhibit its binding to MDM2. As a second generation clinical MDM2 inhibitor, RG7388 has superior potency and selectivity compared to its precursors (e.g. RG7112 and nutlin-3a) (Ding *et al.,* 2013) (Figure 1.6).

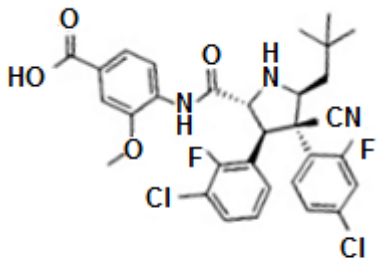

RG7388

Figure 1.6: Chemical structure of RG7388 (adapted from Ding *et al.,* 2013)

p53 is dispensable for RG7388 binding to MDM2. Therefore, p53 mutation status has no effect on RG7388's ability to selectively bind to the p53 binding site of MDM2, stabilise p53 by blocking

its association with MDM2 and effectively activate p53-downstream genes leading to cell cycle arrest and/or apoptosis. RG7388 holds great promise for improving treatments of patients with mutated p53, accounting for half of all human malignancy cases (Hamzehloie *et al.*, 2012). It is currently being tested in multiple clinical trials for solid and haematological tumours (Ding *et al.*, 2013).

1.9 Mechanism and clinical applications of MDM2 inhibition by RG7388

Interaction of the N-terminal TAD1 domain of p53 with the N-terminal hydrophobic pocket (N) of MDM2 triggers a dramatic conformational shift of MDM2 that allows its acidic domain (A) to associate with the ubiquitylation signal in the Box IV/V region of p53. The contact of the C-terminal domain (C) of p53, the RING domain of MDM2 and E2 ligase leads to ubiquitylation of p53 (Meek, 2015). Similar to p53, RG7388 can also trigger a conformational shift of MDM2 (Meek, 2015) (Figure 1.7). Because the different conformations adopted by MDM2 can stabilise and/or induce interactions with its binding partners, the off-target effects of RG7388 remain largely unknown and require thorough investigation (Dastidar *et al.*, 2011; Nicholson *et al.*, 2012; Way *et al.*, 2016).

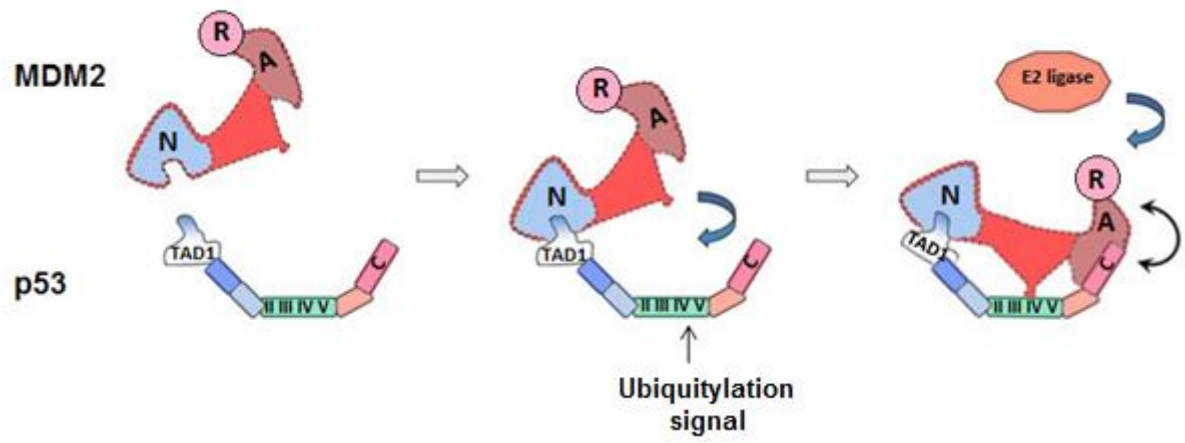

Figure 1.7: Mechanism of p53 ubiquitylation by MDM2 (adapted from Meek, 2015). **N** – N-terminal hydrophobic pocket of MDM2, **A** – acidic domain of MDM2, **R** – RING domain of MDM2, **C** – C-terminal domain of p53.

Although inhibition of MDM2-p53 interaction can efficiently stabilise p53 and activate its downstream signalling, its application in cancer therapy is limited by the off-target toxicity in surrounding normal tissue due to p53 activation. Guided by a crystal structure of the MDM2–MDMX–E2(UbcH5B)–ubiquitin complex, Nomura *et al.,* 2017 designed the MDM2 mutants I440K, I440E and R479P that retain the intact RING-domain but do not interact with ubiquitin-loaded E2 ligase (UbcH5B–Ub). While these mutants are unable to ubiquitinate and degrade p53, they retain the ability to heterodimerise with MDMX, interact with p53 and transcriptionally regulate it (Nomura *et al.,* 2017). Deazaflavin analogues, for example, are small molecule inhibitors targeting the catalytic activity of MDM2 by binding to its RING domain. Co-incubation of these compounds with the full-length MDM2 inhibited its autoubiquitylation and ubiquitylation of p53 (Roxburgh *et al.,* 2012). Therefore, targeting the RING domain of MDM2 to reactivate wt p53 in tumours is a promising strategy for preventing the deleterious side-effects of disrupting the MDM2-p53 interaction in normal tissue. It is also important that MDM2 antagonists do not affect other MDM2 protein–protein interactions.

Aims

The whole-genome sequencing analysis of high-grade MIBC by Cazier *et al*., 2014 revealed a recurring destabilised region on chromosome 12 around *MDM2* gene that is a target of copy number gain in 40 % of analysed MIBC cases. MDM2 amplification often co-occurs with *TP53* mutations suggesting that some of its functions may be p53-independent (Cazier *et al*., 2014). MDM2-NBS1 protein interaction, for example, is reportedly involved in p53-independent negative regulation of DSB repair (Alt *et al.,* 2005). Therapeutic targeting of MDM2 by RG7388 should be investigated to determine whether the tumour suppressive functions of MDM2, both p53-dependent and p53-independent, can be rescued in bladder cancer. RG7388-induced MDM2-inhibition in addition to the bladder preserving treatment with chemoradiation may prove beneficial for patients harbouring *TP53* mutations by radiosensitising cancer cells in p53-independent manner and promoting apoptosis.

The specific aims of this project were to:

1. Validate for T24 and RT112 bladder cancer cell lines earlier reports in the literature suggesting that MDM2 and NBS1 interact in unstressed as well as irradiated cancer cells (Alt *et al.*, 2005; Conradt *et al.*, 2013; Tonsing-Carter *et al.*, 2015).
2. Evaluate the effect of RG7388 alone and in combination with IR on formation of γH2AX foci in T24 and RT112 bladder cancer cell lines.
3. Classify bladder cancer and normal human urothelial cell lines by molecular subtype (basal/luminal) for future studies and identify the CNV status of *NBN* and *MDM2*.

Chapter 2 Materials and methods

2.1 Materials

All chemicals were purchased from Sigma-Aldrich (St. Louis, MO) unless otherwise specified.

2.1.1 Cell lines

Bladder cancer and normal human urothelial cell lines and their clinicopathological features are summarised in Table 2.1.

Table 2.1: Cell lines

Cell line	Disease	Normal/ benign/ malignant	Stage/ grade	Basal/ Luminal	Reference
NHU1754	Normal Human Urothelial primary cell line	N	n/a	n/a	Bentley *et al.*, 2004
253J	Transitional cell carcinoma	M	T4/G4	Intermediate	Fogh *et al*., 1977 Choi *et al.*, 2014
VM-CUB-1	Transitional cell carcinoma	M	G2	Basal	Elliott *et al.*, 1977 Grossman et al., 1986 Choi *et al.*, 2014
HT1376	Transitional cell carcinoma	M	T2/G3	Luminal	Elliott *et al.*, 1977 Fogh et al., 1977 Masters *et al.*, 1986 Choi *et al.*, 2014
5637	Transitional cell carcinoma	M	G2	Basal	Elliott *et al.*, 1977 Fogh *et al*., 1977 Masters *et al.*, 1986 Choi *et al.*, 2014
RT4	Transitional cell papilloma	B	T2/G1	Luminal	Elliott *et al.*, 1977 Fogh *et al*., 1977 Choi *et al.*, 2014
J82	Transitional cell carcinoma	M	T3/G3	Intermediate	Elliott *et al.*, 1977 Fogh *et al*., 1977 Masters *et al.*, 1986 Choi *et al.*, 2014
T24	Transitional cell carcinoma	M	G3	Basal	Bubenik *et al*., 1973 Choi *et al.*, 2015
RT112	Transitional cell carcinoma	M	G2	Luminal	Elliott *et al.*, 1977 Fogh *et al*., 1977 Masters *et al.*, 1986 Williams *et al.*, 2005 Choi *et al.*, 2014

2.1.2 Cell culture media and materials

Bladder cancer cell lines were grown in media supplemented with L-glutamine and foetal bovine serum (FBS; Gibco, Paisley, UK) (Table 2.2). Cells were detached with gamma irradiated 0.12% w/v trypsin-EDTA solution.

Table 2.2: Cell lines and culture media

Cell line	Culture medium
T24, RT112, 5637	RPMI 1640, 10% FBS, 1% L-glutamine
RT4	McCoy's medium, 10% FBS, 1% L-glutamine
J82, HT1376, VM-CUB1	MEM, 10% FBS, 1% L-glutamine, 1% non-essential amino acids
NHU1754	Keratinocyte serum free medium, 50 µg/ml bovine pituitary extract, 0.125 ng/ml recombinant human EGF, 5 µg /ml recombinant human insulin, 0.33 µg/ml hydrocortisone, 0.39 µg/ml epinephrine, 10 µg/ml human holo-transferrin, 0.06 mM $CaCl_2$, 30 ng/ml cholera toxin
253J	DMEM + glutamax: RPMI (50:50), 5% FBS

2.1.3 Buffers and Solutions

Freezing solution

For bladder cancer cell lines, 10% v/v DMSO, 50% v/v FBS and 40% v/v appropriate serum-free medium were mixed together and added to the cell pellet. Normal human urothelial cells were frozen in keratinocyte serum-free medium supplemented with 10% v/v DMSO and 10% v/v FBS. Cells were gently re-suspended in the solution by pipetting, transferred to a 2 ml cryogenic vial and frozen slowly in an isopropanol-containing freezing container at -80°C before being transferred to a liquid nitrogen storage tank.

Non-SDS protein lysis buffer for co-immunoprecipitation

50 mM HEPES

100 mM NaCl (Fisher Scientific, Loughborough, UK)

10 mM EDTA

1% w/v Triton X-100

4 mM sodium pyrophosphate (AppliChem, Darmstadt, Germany)

2 mM sodium orthovanadate

10 mM sodium fluoride

50 mM β-glycerophosphate

pH 7.5

For each co-immunoprecipitation experiment, a new aliquot of protein lysis buffer was used and supplemented with EDTA-free protease inhibitor cocktail (Roche, Mannheim, Germany). For western blotting, this lysis buffer was supplemented with 1% w/v sodium dodecyl sulphate (SDS) (Fisher Scientific, Loughborough, UK).

Laemmli sample buffer

2 X Laemmli sample buffer was purchased pre-made from Sigma-Aldrich (St. Louis, MO)

Phosphate-buffered saline (PBS)

To make up a 1 X solution, two PBS tablets (Gibco, Paisley, UK) were added to 1 litre of dH_2O. The solution was then autoclaved.

Blocking buffer for Western blotting

PBS-Tween 0.05% v/v (PBST) was mixed with Li-Cor blocking buffer (Li-Cor Biosciences UK Ltd, Cambridge, UK) 1:1 v/v.

1 X Running buffer for electrophoresis

0.1M Tris base (Fisher Scientific, Rockford, IL)

0.1% w/v SDS

0.1 M HEPES

pH 8.6

1 X Transfer buffer for electrophoresis

25 mM Tris base

192 mM glycine (Fisher Scientific, Rockford, IL)

20% v/v methanol (Fisher Scientific, Rockford, IL)

pH 8.3

Fixation solution for immunofluorescence

1:1 solution of methanol: acetone (Fisher Scientific, Loughborough, UK)

Fresh solution was made for each experiment and pre-chilled at -20°C prior to use.

Blocking solution for immunofluorescence

2.5 g BSA (Europa Bioproducts, Cambridge, UK)

50 ml PBS (Gibco, Paisley, UK)

50 µl Triton X-100

The fresh solution was made for each experiment and pre-chilled at 4°C prior to use.

Chemotoxic agents

RG7388 was purchased from BioVision (San Francisco, CA) and dissolved in DMSO to a 10 mM stock concentration. Single-use aliquots were stored at -20°C.

2.2 Methods

2.2.1 Cell Culture

Bladder cancer cell lines were cultured in T75 flasks in 10 ml of FBS-supplemented growth medium. The growth medium, as specified in Table 2.2, was warmed to 37°C in a water bath, then medium in flasks removed by aspiration, and 3 ml 0.12% trypsin-EDTA added to the cell monolayer for 3-6 minutes incubation at 37°C in 5% CO_2 to allow for detachment of the cells. Growth medium was added (1:1) and mixed and the cells transferred to a plastic centrifuge tube. Cells were pelleted by centrifugation in Heraeus Labofuge 400 centrifuge (Thermo Fisher Scientific, Waltham, MA) at 1,300 rpm (200 g) for 3 minutes. The pellets were then resuspended in 10 ml of fresh growth medium and passaged in a 1:3 ratio.

Normal human urothelial (NHU1754) cells were cultured in keratinocyte serum free medium (KSFM). Following the aspiration of growth medium, the NHU1754 cells were incubated with 0.1% EDTA in PBS for 10 minutes at 37°C. After EDTA aspiration, the cells were coated with Trypsin Versene and incubated at 37°C for 3-5 minutes. To inhibit trypsin, 1% trypsin inhibitor (1:10 v/v) was used. The cells were then transferred into a Sterilin Universal conical tube, centrifuged at 350 g for 4 minutes and passaged in 1:3 ratio in 6 ml medium in a T25 (25 cm^2) tissue culture flask.

2.2.2 Irradiation of cells

A Caesium-137 γ-ray source (GSR D1, Gamma-Service Medical GmbH, Leipzig, Germany) was used at a dose-rate of 1.7 Gy per minute. Cells were irradiated in 10 cm dishes to a total dose of 5 Gy at room temperature and then immediately transferred to the 37°C incubator.

2.2.3 Chemosensitivity clonogenic assays

The cytotoxic effect of RG-7388 on tumour cells was assessed by a chemosensitivity clonogenic assay. Seventy per cent confluent cells in 10 cm dishes in 10 ml medium were exposed to appropriate increasing concentrations of the drug (1 nM – 2 μM) for 24 hours. The next day, the medium was aspirated, and the dishes washed twice with 10 ml warm, sterile PBS, the cells were trypsinised and plated at a density of 700 cells per plate for each drug concentration. Finally, 10 ml of fresh medium was added to each dish and the dishes were incubated at 37°C in 5% CO_2.

Eight or fourteen days later (eight for T24, fourteen for RT112) the medium was decanted from all dishes and replaced with 93% methanol: 7% acetic acid to both wash and fix colonies for 10 minutes. After fixing the colonies, 5 ml of Brilliant Blue R Concentrate (0.25% Brilliant blue R: 40% methanol: 7% acetic acid) diluted 1:1 with distilled H_2O, was added for 30 minutes to stain colonies. The stain was poured away and the dishes were rinsed with running water before being left to dry overnight. The colonies of ≥ 50 cells were counted automatically using an Oxford Optronix Colcount (Oxford Optronix, Oxford, UK).

A similar protocol was used to assess the radiosensitising effect of RG7388. Twenty-four hours after treatment, the cells were plated at an appropriate density (700-2100 per 10 cm dish) and irradiated with 0-8 Gy IR. Following exposure to IR, 10 ml of fresh medium was added to each dish and the dishes were incubated at 37°C in 5% CO_2 for eight or fourteen days.

2.2.4 Western blotting

2.2.4.1 Preparation of cell lysates

Cells were seeded at a density of 1 x 10^6 cells/ml in 10 ml of medium in 10 cm dishes. The next day dishes were treated with RG7388 (or DMSO vehicle control), as necessary. After 24 hours of incubation, cells from the dishes were scraped in ice-cold PBS and lysed with protein lysate buffer containing 1% w/v SDS, using a volume approximately equal to the volume of the cell pellet (typically 50 µl), supplemented with 0.1 g/ml protease inhibitor Complete Mini (Roche, Mannheim, Germany). The samples were then sonicated 5 times with a probe sonicator, 3 seconds per pulse, on ice in 1.5 ml microcentrifuge tubes. Sonicated pellets were left for a further 5 minutes on ice and then centrifuged for 7 minutes at 14,000 rpm (19,000 g) in an Eppendorf centrifuge 5430R (Eppendorf, Hamburg, Germany), pre-cooled to 4°C.

2.2.4.2 Protein concentration measurement

Protein concentration was quantified by bicinchoninic acid (BCA) assay (Pierce). First, 10 µl of a dilution series (0.1 to 2 mg/ml) of bovine serum albumin standard and 2 µl of the lysed protein samples were loaded onto a 96-well plate (Corning Inc., Corning, NY). Next, reagents A and B from the assay kit (1: 5 v/v) (Thermo Scientific, Rockford, IL) were added to each well, and the plate incubated for 45 minutes at 37°C. Following incubation, absorbance was measured at 562 nm with a POLARstar Omega plate reader. The protein concentration of each sample was then calculated by plotting the linear regression curve of absorbance against the dilution series of bovine serum albumin.

2.2.4.3 Sample preparation

Fifty micrograms of the protein lysates were mixed with equal volumes of 2 x Laemmli sample buffer and heated on an Accublock Digital Dry Bath from Labnet International Inc. (Edison, NJ) at 95°C for 5 minutes.

2.2.4.4 Electrophoresis, western blot and incubation with antibodies

The samples were loaded on a 10% acrylamide gel with Amersham Full Range Rainbow Marker lane (GE Healthcare Life Sciences, Little Chalfont, UK) and run at 100 V for 1 hour to separate samples according to their molecular weight. Next, the gel was soaked in ice cold transfer buffer for 5 min. Proteins were then transferred from the gel onto a nitrocellulose membrane with 0.45 µm pores (Thermo Scientific, Rockford, IL) for two hours at 40 V. The membrane was placed in 10 ml membrane blocking buffer for 30 minutes on a mini gyro-rocker SSM3 (Stuart, Stone, UK), at 24 revolutions per minute (RPM), and then incubated with primary antibody overnight at 4°C on a See-saw rocker SS24 (Stuart, Stone, UK), at 24 RPM (Table 2.3). The following day, the membrane was washed for 10 minutes three times in 0.05% PBST and incubated in secondary fluorochrome-conjugated (Li-Cor Biosciences UK Ltd., Cambridge, UK) mouse or rabbit antibody (1:5000) for one hour at room temperature on a mini gyro-rocker (Table 2.3). The membrane was washed again three times, 10 minutes each, in PBS-T. Finally, the membrane was scanned using an infrared Li-Cor Odyssey detection system, with the linear range pixel count (Li-Cor Biosciences UK Ltd., Cambridge, UK). Each experiment was performed in triplicates. All antibodies were diluted in 50% PBST and 50% Li-Cor blocking buffer.

Table 2.3: Antibodies used for western blotting, co-immunoprecipitation and immunofluorescence staining

Antibody target	Primary/ Secondary	Source (clone)	Dilution	Specificity
Anti-rabbit IgG HRP-linked	Primary	Cell Signalling #7074	1:1000	Rabbit
β-actin	Primary	Abcam ab8226	1:10000	Mouse
MDM2	Primary	GeneTex GTX16895 (2A10)	1:250	Mouse
MRE11	Primary	Novus Biologicals NB100-142	1:5000	Rabbit
Conjugated ubiquitin chain (FK2)	Primary	Cayman Chemical #14220 (FK2)	1:1000	Mouse
NBS1	Primary	Novus Biologicals NB100-143	1:1000	Rabbit
p53	Primary	Santa Cruz sc-126 (DO-1)	1:250	Mouse
RAD50	Primary	Cell Signalling #3427	1:1000	Rabbit
IRDye 680LT	Secondary	Licor P/N 925-68021	1:5000	Rabbit
IRDye 800CW	Secondary	Licor P/N 925-32210	1:5000	Mouse
Alexa Fluor 488	Secondary	Thermo Fisher Scientific (A-11001)	1:5000	Mouse
Alexa Fluor 568	Secondary	Thermo Fisher Scientific (A-11011)	1:5000	Rabbit

2.2.5 Co-immunoprecipitation

Cell pellets of approximately 3 x 10^6 cells were lysed in 200 µl of non-SDS lysis buffer. The sonicated lysates were centrifuged at 14,000 rpm for 8 minutes at 4°C and supernatant transferred to a clean 1.5 ml tube. Protein lysates were pre-cleared for non-specific protein binding by incubating with 10 µl magnetic protein A/G Dynabeads (Novex, Life Technologies) for 1 hour at 4°C, with rotation. Samples were then placed in a DynaMagSpin magnetic holder and the supernatant transferred into a clean 1.5 ml tube. Lysate was incubated with a primary antibody (Table 2.3) overnight at 4°C, with rotation. Thirty micrograms of pre-cleared protein lysate was retained to act as a whole cell extract control. MDM2 and NBS1 proteins were pulled down from three hundred micrograms of pre-cleared lysate.

2.2.6 Immunofluorescence microscopy and analysis of γH2AX, NBS1 and MDM2 foci

Ionising radiation-induced γH2AX focus formation was used as a surrogate marker for DNA damage (Kuo and Yang, 2008). For the immunofluorescence experiments, 2.5 x 10^5 cells were plated onto sterile glass coverslips in 5 cm dishes in 3 ml culture medium, and the following day treated with DMSO or RG7388 for 24 hours. Then, cells were either fixed or irradiated with 5 Gy prior to fixation, at required time points. Cells were fixed and permeabilised by incubation in a 1:1 (v/v) ice-cold mixture of methanol and acetone at -20°C, followed by three PBST washes. Following blocking for 30 minutes at room temperature in 5% BSA, the coverslips were incubated overnight at 4°C with primary antibodies diluted in 5% BSA and 0.1% Triton (Table 2.3).

The following day, the coverslips were washed three times in PBST for 10 minutes with shaking, and incubated with secondary antibodies for 1 hour (Table 2.3). Then, the coverslips were washed three more times in PBST for 10 minutes with shaking and mounted onto slides with Fluoromount G containing 0.1 µg/ml DAPI. The slides were left to dry in the dark overnight and then scanned using a Zeiss LSM 780 confocal microscope. For each condition three slides were prepared independently and 100 cells counted per slide.

2.2.7 Quantitative RT-PCR

2.2.7.1 RNA extraction

Total RNA was extracted from T24 and RT112 bladder cancer cell lines, at a seeding density of 1 x 10^6 cells per 10 cm dish, following treatment with RG7388, 5 Gy IR or a combination of the two. The cells were trypsinised, pelleted and the RNA was extracted using the RNeasy Plus Mini kit, according to the manufacturer's protocol (Qiagen, Hilden, Germany). The concentration of purified RNA was determined using a Nanodrop spectrophotometer (Thermo Scientific, Wilmington, DE).

2.2.7.2 Complementary DNA synthesis

Complementary DNA (cDNA) was generated from 5 µg RNA, using a high capacity cDNA reverse transcription kit (Applied Biosystems, Foster City, CA) as per manufacturer's instructions. The RNA was made up to a total volume of 10 µl with RNAse-free dH_2O (Qiagen, Hilden, Germany). The final reaction volume was 20 µl.

Reagent	**Volume (µl)**
10X RT buffer	2.0
25X dNTP (25 µM)	0.8
Oligo random primers	2.0
RT enzyme (MultiScribe reverse transcriptase, 50 U/µl)	1.0
5 µg RNA	10.0
RNase-free dH_2O	4.2
Total	20

Temperature (°C)	**Time (min)**
25	10
37	120
85	5
4	∞

2.2.7.3 Primer design for qPCR

Primers were designed using IDT primerQuest software (available from www.idtdna.com/primerquest/Home/Index) to amplify the coding regions of human *MDM2* (CCDS ID: CCDS61189.1. Accessed January 2017) and *NBN* (CCDS ID: CCDS6249.1. Accessed January 2017) (Hubbard *et al.,* 2002)

Primer name	Primer sequence (5'-3')	Tm (°C)
MDM2 forward	GGGAGAGTGATACAGATTCAT	57.0
MDM2 reverse	GTTGCAATGTGATGGAAGG	61.6
NBN forward	TCCATCTGGCATAAATGATGA	62.8
NBN reverse	GTGGAAGTTTTCCTGCTCCA	64.1

2.2.7.4 Quantitative qRT-PCR

Quantitative PCR (qPCR) was performed using SYBR Green PCR Master Mix (Applied Biosystems, Warrington, UK). The components were combined in a final volume of 50 µl and run on a 7500 Fast Real-Time PCR System thermal cycler (Applied Biosystems, Foster City, CA) under the conditions suggested by the manufacturer.

Reagent	Volume (µl)
100 ng cDNA	1
SYBR Green PCR Master Mix	20
Nuclease-free dH_2O	25
10 µM forward primer	2
10 µM reverse primer	2
Total	50

Temperature (°C)	Time	Cycles
95	30 sec	1X
95	15 sec	
55	15 sec	40X
68	3 min	
68	7 min	1X
4	∞	1X

2.2.8 Copy Number Analysis

2.2.8.1 SNP array hybridisation

The genomic DNA (gDNA) extracts were kindly provided by Dr Eva McGrowder. Genomic DNA samples were hybridised to a ~300K Human CytoSNP-12 BeadChip (Illumina Inc, San Diego, CA) by Genomics Core at Wellcome Trust Centre for Human Genetics. The preliminary data analysis was carried out by Dr Samantha Knight using Nexus Discovery Edition v6.1 (BioDiscovery, Hawthorne, CA) with the following settings in the first instance (SNPRank Segmentation): Significance Threshold 1x 10-7; Max Contiguous Probe Spacing (Kbp) 500.0; Min number of probes per segment 3; High Gain 0.4; Gain 0.15; Loss -0.15; Big Loss -1.0; 3:1 sex chromosome gain 1.2; Homozygous Frequency threshold 0.97; Homozygous Value Threshold 0.90; Heterozygous Imbalance Threshold 0.45; Minimum LOH Length (Kb) 1000; percentage outliers to remove 3%. My responsibilities included subsequent confirmation and curation of the copy number abnormality (CNA) calls.

2.2.8.2 Reporting Copy Number Abnormalities (CNAs) and Copy Neutral Loss of Heterozygosity (cnLOH)

Nexus-processed LogR and B-Allele frequency (BAF) plots were inspected visually and manually curated to ensure a high level of confidence in the results. CNA events that had been repeatedly observed previously either in negative control data (i.e. genomic alterations in disease-free tissue samples) deposited in the database of genomic variants (DGV) (MacDonald *et al.*, 2014) or in in-house datasets were excluded from subsequent analyses. This minimised the inclusion of common germline events in the absence of germline DNAs with which to compare data. All CNAs and copy neutral loss of heterozygocity (cnLOH) regions ≥ 2 Mb were recorded. The current project is a follow-up from the whole-genome sequencing of bladder cancers study by Cazier *et al.,* 2014. Therefore, a similar size threshold of ≥2Mb for cnLOH was applied. Any smaller regions

of homozygosity occur more frequently with their physiological roles being poorly understood. Therefore, including them in the CNV analysis would create huge amounts of hard-to-filter data and make further investigation of their clinical relevance unreliable (Cazier *et al.,* 2014). Manually verified calls, together with relevant gene information, were exported to Microsoft Excel for analysis of possible associations between the molecular subtype of the bladder cancer cell lines and CNA events.

2.2.9 Statistical analysis

GraphPad Software (San Diego, CA) was used for statistical comparison between two groups of samples (e.g. treated vs. untreated control) using unpaired student's t-test. All data was expressed as mean values ± standard error of the mean. P values smaller than 0.05 were considered statistically significant.

Chapter 3 Results

3.1 Copy number variation analysis of *MDM2* and *NBN* genes.

Loss of the tumour suppressor p53 function is a molecular signature of many malignancies (Strano *et al.*, 2007). It drives tumour development by triggering genomic instability and insensitivity to pro-apoptotic signals. MDM2 is an E3 ubiquitin ligase often overexpressed in human and murine cancers, including bladder cancer (The Cancer Genome Atlas Research Network, 2014; Van Allen *et al.*, 2014). Upregulated MDM2 targets p53 for proteasomal degradation and inhibits the induction of the p53-mediated checkpoints that constitute a barrier to tumour progression (Meek, 2015).

Therefore, it is not surprising that the *MDM2* copy number gain, reported in 9% of bladder cancer cases, often co-occurs with copy number alterations or truncating protein-inactivating mutations of *TP53* (Carrillo *et al.*, 2015; Guo *et al.,* 2013; Appendix 2). However, the copy number abnormalities of *MDM2* are also known to co-occur with copy number alterations or protein-inactivating mutations of *NBN* (Figure 3.1) (Guo *et al.*, 2013; The Cancer Genome Atlas Research Network, 2014; Van Allen *et al.*, 2014). MDM2 and NBS1 are reported to directly interact with each other and are recruited in the same signalling pathway inhibiting DNA repair in a p53-independent manner. However, the nature of the causal link between tumorigenesis, upregulation of *MDM2* and copy number alterations of *NBN* remains uncertain (Guo *et al.*, 2013; Cazier *et al.*, 2014; The Cancer Genome Atlas Research Network, 2014; Kim *et al.*, 2015) (Figure 3.1).

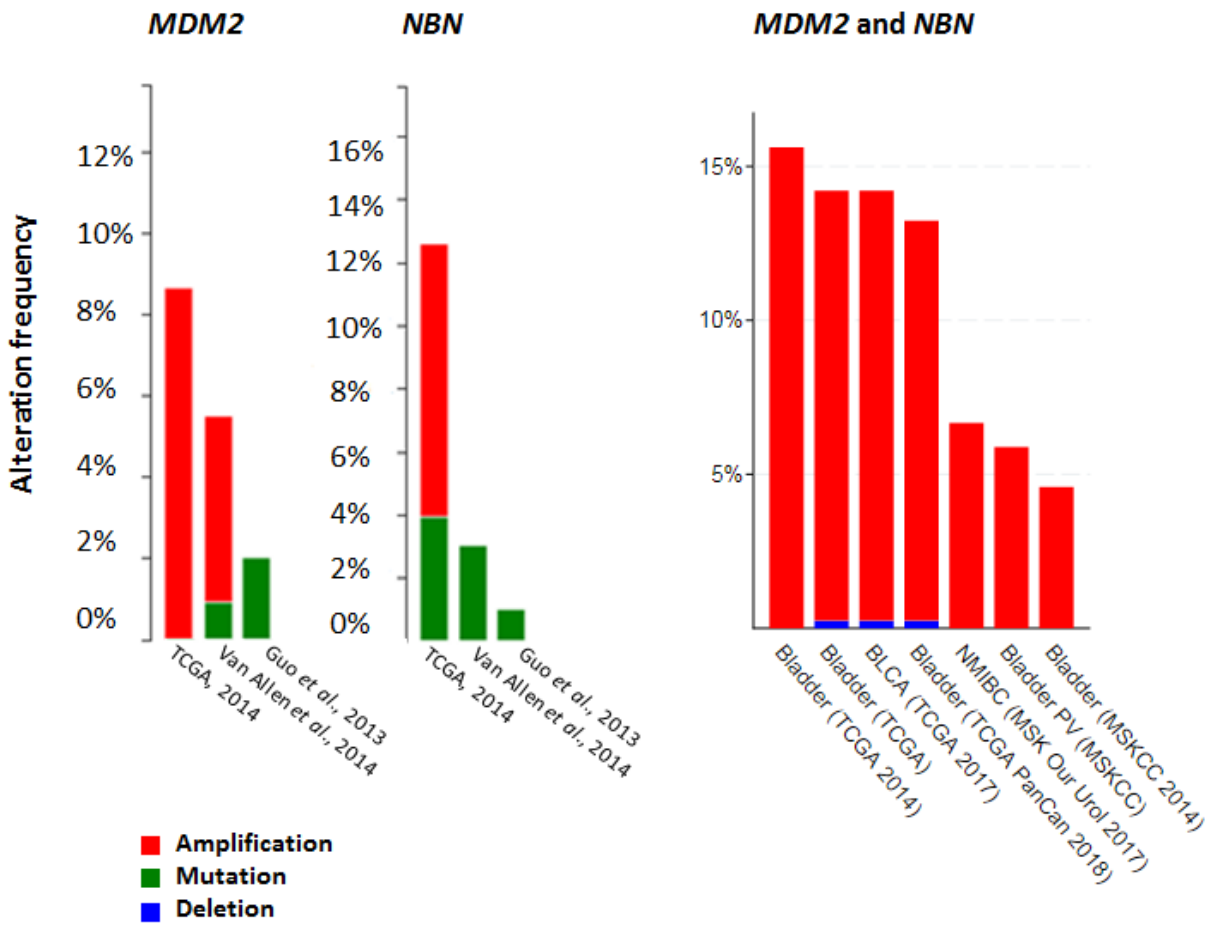

Figure 3.1: Summary of copy number alteration and mutation incidence for *MDM2* and *NBN* genes in bladder cancer clinical studies available via the cBioPortal for Cancer Genomics (http://www.cbioportal.org/) (Guo *et al.*, 2013; The Cancer Genome Atlas Research Network, 2014; Van Allen *et al.*, 2014).

3.2 Copy number variation analysis in bladder cancer and NHU cell lines

The preliminary results of CNA analysis of *NBN* and *MDM2* in bladder cancer and normal human urothelial cell lines are summarised in Tables 3.1-3.2 and Appendix 1. In bladder cancer cell lines, copy number alteration (CNA) and copy-neutral loss of heterozygosity (cnLOH) events clustered in a molecular subtype-specific way. Basal and p53-like subtypes are often characterized by cnLOH of *MDM2* and *NBN*, whereas both bladder cancer cell lines with luminal phenotypes demonstrated CN gain of *NBN*, which co-occurred with *MDM2* CN gain in the RT112 cell line. Copy number variation analysis in eight bladder cancer and one normal human urothelial cell lines was performed using Nexus Copy Number software (El Segundo, CA).

Table 3.1: *NBN* CNA events in bladder cancer and normal human urothelial cell lines

Cell line	Phenotype	Chromosome region	Length (bp)	*NBN CNA events*
T24	Basal	chr8:46,942,842-146,364,022	99421181	cnLOH
VM-CUB-1	Basal	chr8:82,400,539-146,364,022	63963484	cnLOH
5637	Basal	None observed	None observed	None observed
253J	p53-like	chr8:46,942,842-146,364,022	99421181	cnLOH
HT1376	p53-like	chr8:79,887,906-92,953,667	13065762	CN gain
J82	p53-like	chr8:46,942,842-124,025,219	77082378	cnLOH
RT112	Luminal	chr8:46,942,842-146,364,022	99421181	CN gain
RT4	Luminal	chr8:46,933,082-146,364,022	99430941	cnLOH
NHU1754	Normal	None observed	None observed	None observed

Table 3.2: *MDM2* CNA events in bladder cancer and normal human urothelial cell lines

Cell line	Phenotype	Chromosome region	Length (bp)	*MDM2 CNA events*
T24	Basal	chr12:38,645,225-133,851,895	95206671	cnLOH
VM-CUB-1	Basal	chr12:65,697,091-107,559,140	41862050	cnLOH
5637	Basal	chr12:38,088,091-133,851,895	95763805	cnLOH
253J	p53-like	chr12:38,094,338-133,851,895	95757558	cnLOH
HT1376	p53-like	chr12:52,267,011-133,851,895	81584885	cnLOH
J82	p53-like	chr12:38,094,338-133,851,895	95757558	cnLOH
RT112	Luminal	chr12:38,094,338-133,851,895	95757558	CN gain
RT4	Luminal	chr12:58,072,811-133,851,895	75779085	CN gain
NHU1754	Normal	None observed	None observed	None observed

3.3 Determination of the IC_{50} dose of RG7388 for T24 and RT112 cell lines

The cytotoxicity of RG7388 which binds MDM2 at the p53 binding site (18-101 aa) was assessed in T24 and RT112 bladder (T24: mutant p53, RT112: wild type p53) cancer cell lines by undertaking clonogenic assays with a range of concentrations 0-10 µM. The estimated IC_{50} value was 1 µM for T24 and 2 µM for RT112 were used for all further experiments as higher concentrations of RG7388 were toxic to the cells (Figure 3.2).

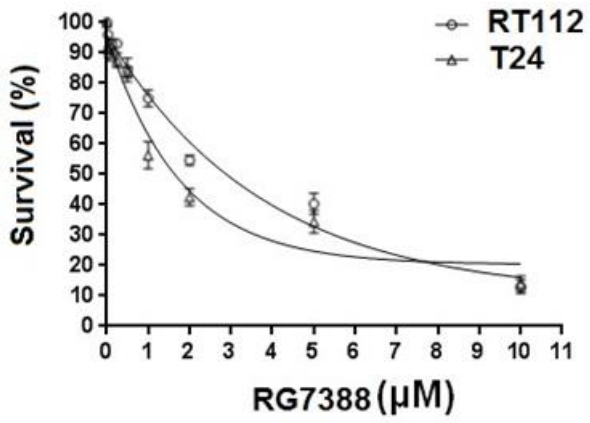

Figure 3.2: Evaluation of RG7388 cytotoxicity in bladder cancer cell lines by clonogenic assay. The experiment was done with three technical replicates per treatment. Error bars represent the standard error of the mean.

3.4 RG7388 activates the DNA damage response but does not act as a radiosensitiser

In order to evaluate the ability of RG7388 to trigger the DNA damage response in T24 and RT112 cells, γH2AX foci formation was analysed following exposure to 5 Gy IR, IC_{50} dose of RG7388 and a combination of the two. γH2AX foci were detected in T24 and RT112 cells after 24-hour treatment with RG7388 alone, suggesting that this agent may contribute to initiation of the DNA damage response (Figure 3.3 - 3.4).

Consistent with earlier published studies (Valentine *et al.,* 2011), the greater effect of combination treatment with RG7388 and radiation reported in xenograft models of childhood sarcoma was also seen in T24 and RT112 cells treated with RG7388 and 5 Gy IR. The highest

number of γH2AX-positive nuclei was detected in both cell lines following combination treatment compared to untreated controls ($p < 0.01$). The unpaired t-test showed statistically significant differences in the number γH2AX-positive nuclei between different treatment regimens and treated vs untreated samples, for both cell lines (Figure 3.5). However, the radiosensitivity clonogenic assays suggest that under the treatment conditions of this study, the IC_{50} dose of RG7388 does not have a significant radiosensitising effect in T24 and RT112 cells (p = n.s.) (Figure 3.6).

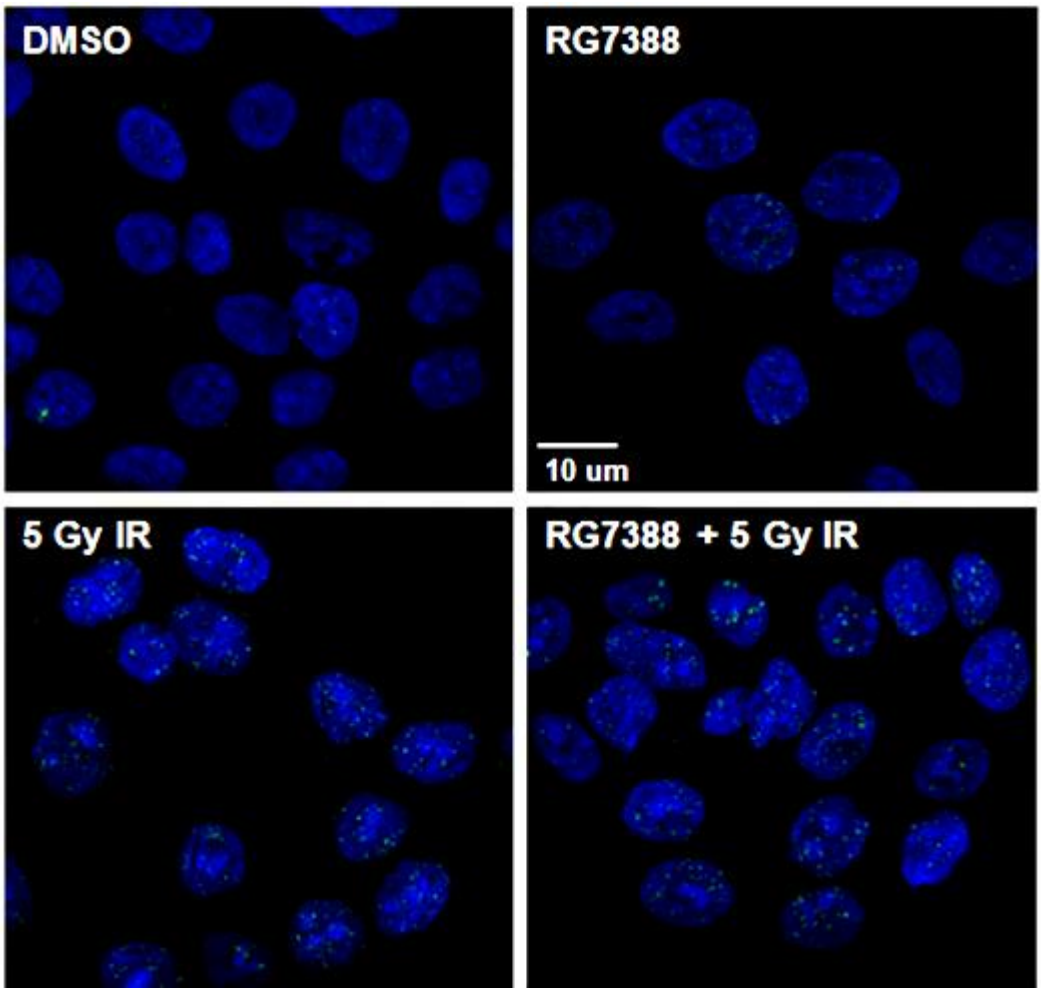

Figure 3.3: γH2AX foci analysis in RT112 cells treated with DMSO + 0 Gy IR, 2 µM RG7388 + 0 Gy IR, DMSO + 5 Gy IR and 2 µM RG7388 + 5 Gy IR, stained for γH2AX and counterstained for DAPI four hours after exposure to IR. Nuclei with ≥ 4 foci were considered γH2AX – positive. Number of foci between different treatment regimens was estimated by unpaired t-test. The foci were counted using the ImageJ software with a minimum threshold of ≥5 foci per cell nucleus.

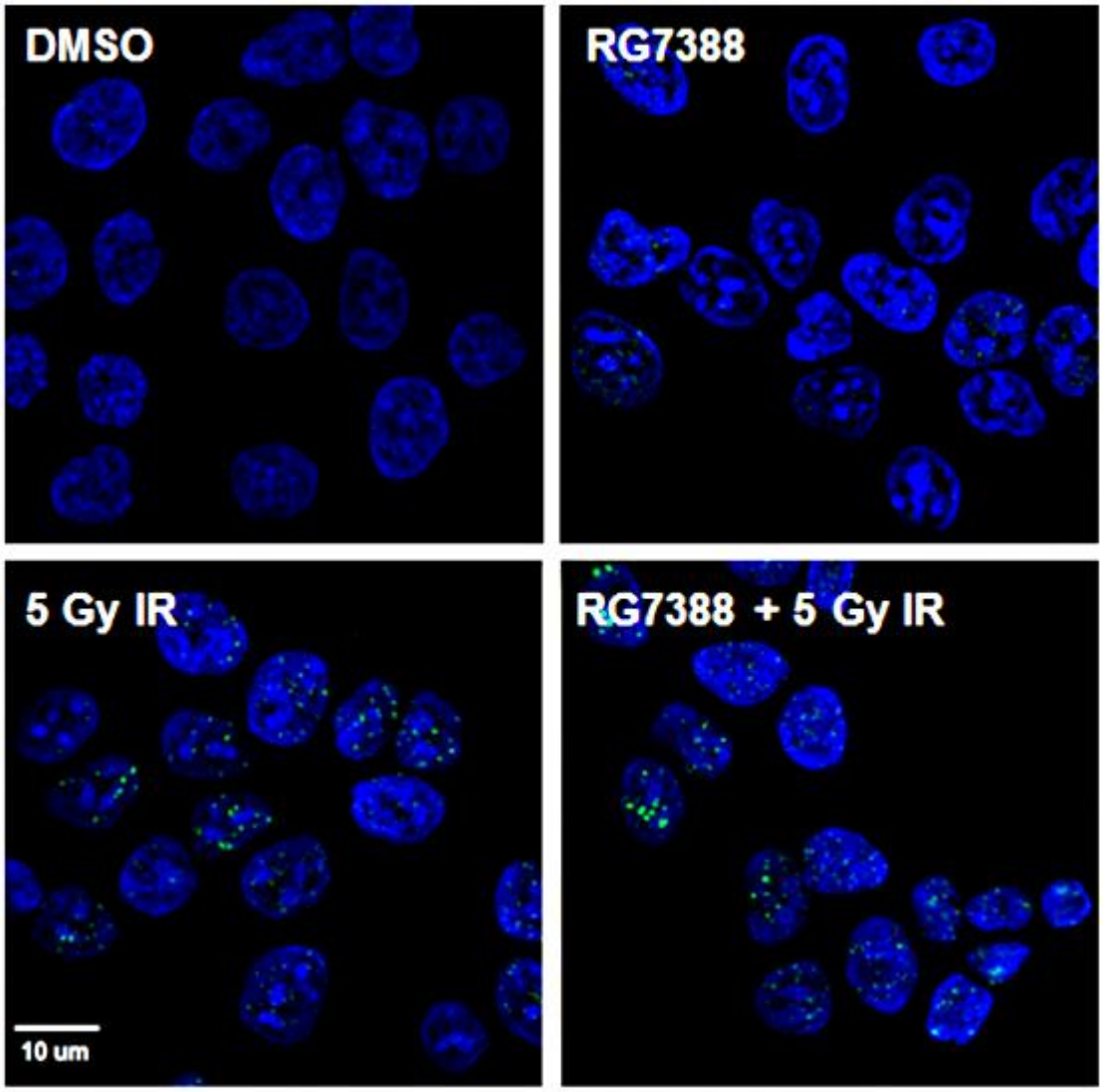

Figure 3.4: γH2AX foci analysis in T24 cells treated with DMSO + 0 Gy IR, 1 µM RG7388 + 0 Gy IR, DMSO + 5 Gy IR and 1 µM RG7388 + 5 Gy IR, stained for γH2AX and counterstained for DAPI four hours after exposure to IR. Nuclei with ≥ 4 foci were considered γH2AX – positive. Number of foci between different treatment regimen was estimated by unpaired t-test. The foci were counted using the ImageJ software with a minimum threshold of ≥5 foci per cell nucleus.

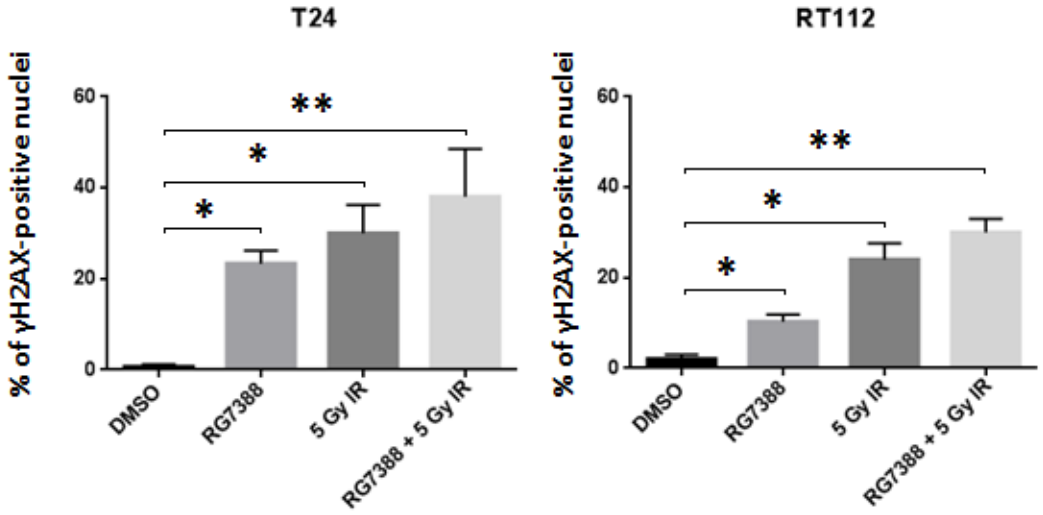

Figure 3.5: Quantitative analysis of γH2AX-positive nuclei per 100 cells by unpaired student t-test. T24 and RT112 cells were treated with DMSO + 0 Gy IR, IC_{50} RG7388 + 0 Gy IR, DMSO + 5 Gy IR and IC_{50} RG7388 + 5 Gy IR, stained for γH2AX and counterstained for DAPI four hours after exposure to IR. * $p < 0.05$; ** $p < 0.01$. Error bars represent standard error of the mean.

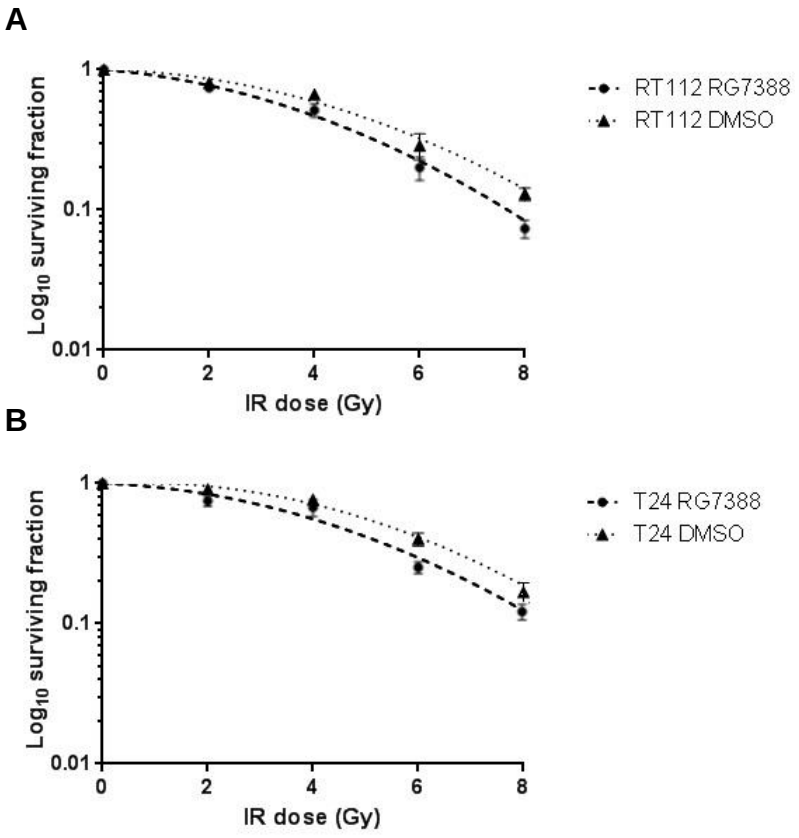

Figure 3.6: Radiosensitivity clonogenic assay of A: RT112 and B: T24 cell lines treated with 0-8 Gy IR +/- IC_{50} dose of RG7388. The experiment was performed with three technical replicates per treatment. Error bars represent standard error of the mean.

3.5 RG7388 and IR treatment causes significant changes in MDM2 but not NBS1 mRNA expression

To evaluate whether RG7388, IR and a combination of the two would influence the expression of *MDM2* and *NBN* genes, a qPCR experiment was undertaken with mRNA extracted from T24 and RT112 cells following three treatment regimens. There is a trend for upregulation of MDM2 with IR in both cell lines and downregulation with RG7388, which is only occurring in T24 but not RT112 cell line. The difference in mRNA expression levels of *MDM2* in untreated T24 cells vs treated with 5 Gy IR is statistically significant ($p < 0.01$). The same is true for T24 treated with 5 Gy (IR) vs 5 Gy (IR) + 1 µM RG7388 ($p < 0.01$) and 5 Gy (IR) vs 5 Gy (IR) + 2 µM RG7388 ($p < 0.01$). In RT112 cells, statistically significant upregulation of *MDM2* we detected in untreated vs 2 µM RG7388 ($p < 0.01$), untreated vs 5 Gy (IR) + 1 µM RG7388 ($p < 0.01$) and untreated vs 5 Gy (IR) + 2 µM RG7388 ($p < 0.01$) (Figure 3.7 A-B).

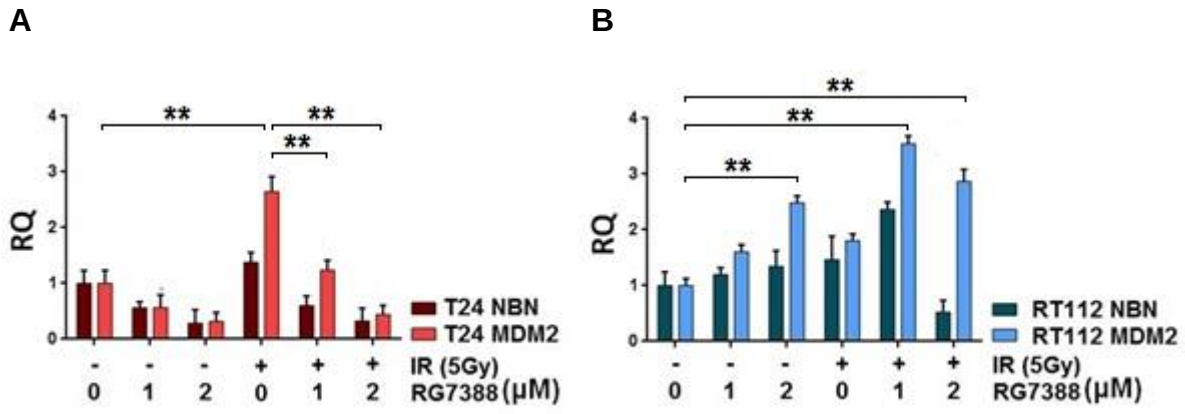

Figure 3.7: Evaluation of *NBN* and *MDM2* mRNA expression by SYBR green real-time qPCR. A: T24, B: RT112. ** $p < 0.01$. The experiment was performed with three technical replicates per treatment. Error bars represent standard error of the mean.

3.6 RG7388 and IR treatment alters the protein levels of MDM2 but not NBS1

To determine whether IR-induced DNA damage, treatment with RG7388 or a combination of the two would affect the protein levels of MDM2 and NBS1, whole cell lysates (30 µg) of T24 and RT112 cells following 24-hour treatment with RG7388 and/or four hours after their exposure to

5 Gy IR were immunoblotted for endogenous NBS1, MDM2 [2A10] and β-actin as a loading control. No statistically significant difference in NBS1 protein levels was detected in T24 and RT112 following treatment with RG7388, 5 Gy IR or a combination of the two compared to untreated cells (p = n.s.) (Figure 3.8 A-F). However, there is a statistically significant trend of elevating MDM2 protein levels in RG7388 vs untreated ($p < 0.01$) and RG7388 + 5 Gy (IR) vs untreated ($p < 0.01$). The fact that the protein level of MDM2 in RT112 cells does not decrease following exposure to IR compared to untreated controls may be partly caused by the increased copy number of MDM2 in this cell line. This effect has previously been reported in cells of diverse tissue origins (Perry et al., 2004; Zhang *et al.,* 2000). Additionally, MDM2 is known to be an important component of cell responses to IR treatment for it down-regulates the pro-apoptotic activity of p53 in surviving cells. Decreased levels of MDM2 sensitize cells to ionizing radiation. This finding is also consistent with earlier published studies (Carrillo *et al.*, 2015) suggesting that nutlin-family small molecule inhibitors of MDM2 increase the protein levels of MDM2 by stabilising its N-terminal hydrophobic p53 binding pocket. Future experiments could include negative controls such as MDM2 CRISPR KO or KD cell line or MDM2 with point mutation(s) in the N-terminal p53-binding site, blocking its interaction with RG-7388.

In RT112 cell line, the protein levels of MDM2 appeared higher compared to NBS1 regardless of the treatment regimen. Future experiments should also involve cyclohexamide treatment in order to be able to inhibit the protein synthesis and determine the half-life of MDM2 and NBS1.

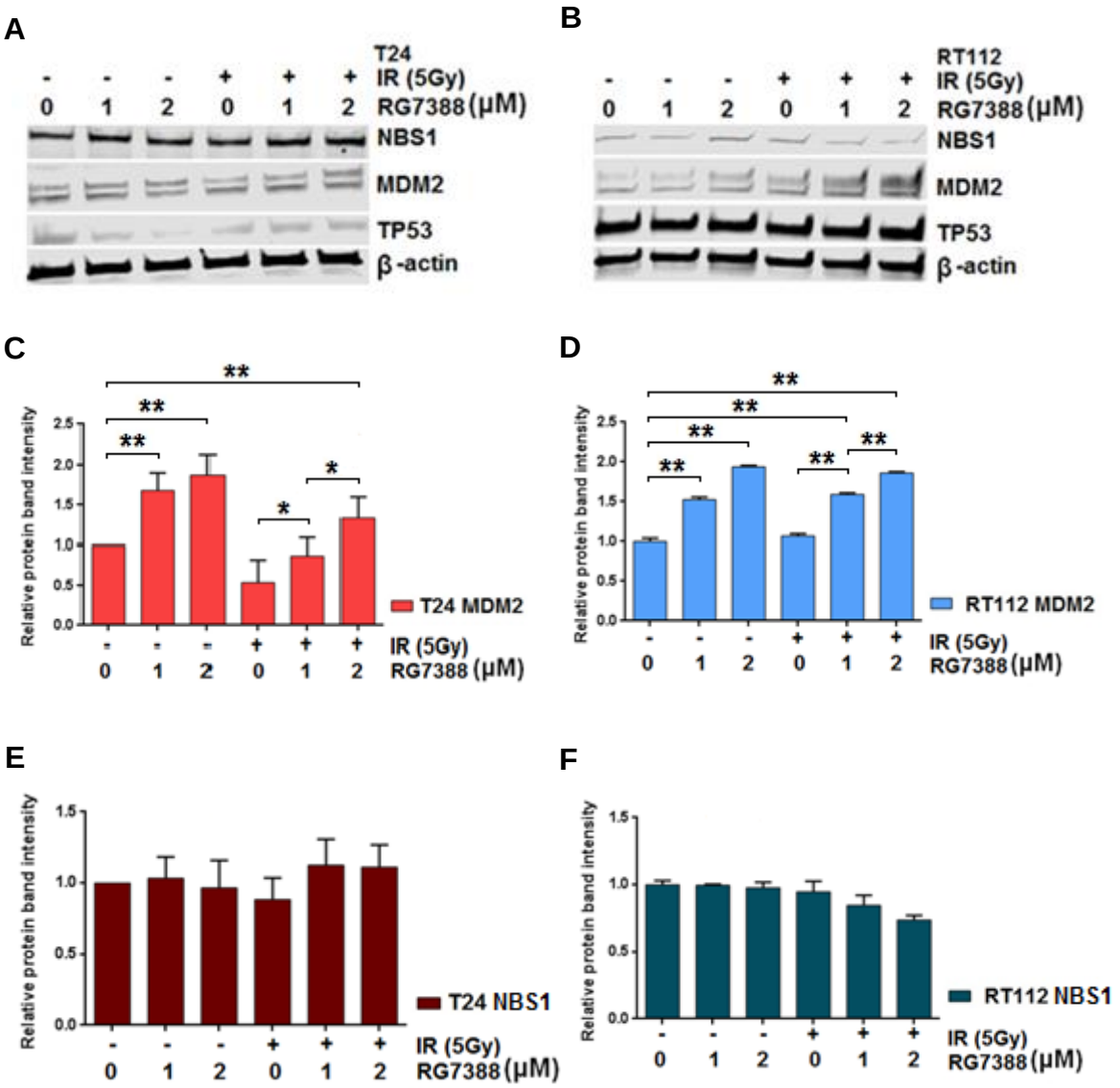

Figure 3.8: A, B: RG7388 and 5 Gy IR effect on MDM2 and NBS1 protein levels analysed by western blot. **C, D:** Quantitative analysis of MDM2 protein levels in T24 and RT112 cell lines. **E, F:** Quantitative analysis of NBS1 protein levels in T24 and RT112 cell lines. * $p < 0.05$; ** $p < 0.01$. The experiment was performed with three technical replicates per treatment. Error bars represent standard error of the mean.

3.7 In the nuclei of cells exposed to 5 Gy IR, NBS1 and MDM2 co-localise without foci formation

The spatiotemporal dynamics of MDM2 and NBS1 protein localisation and the effect of IR-induced DNA damage were analysed by immunofluorescence staining. Non-irradiated T24 and RT112 cells were fixed and then co-stained with NBS1-specific (red) and MDM2-specific (green) antibodies (Figure 3.9-3.10, top panels). T24 and RT112 cells treated with 5 Gy IR were fixed 4-48 hours post-irradiation and then co-stained with NBS1-specific (red) and MDM2-specific (green) antibodies (Figure 3.9-3.10, the remaining panels).

Merging the images revealed regions of overlap, which indicate co-localisation of MDM2 and NBS1 in the presence of IR-induced DNA damage and in untreated controls. In non-irradiated cells, MDM2 is expressed throughout the cell, whereas the localisation of NBS1 is predominantly nuclear. Four hours following exposure to 5 Gy IR, a large fraction of cytoplasmic MDM2 translocated to the nucleus and some of it co-localised with NBS1. Twenty four hours following IR treatment, when the majority of dsDNA lesions have been repaired, some of MDM2 translocated back to the cytoplasm while NBS1 remained predominantly nuclear. Forty-eight hours post-IR NBS1 localisation remained mostly nuclear and translocation of MDM2 to the nucleus continued. NBS1 and MDM2 are known as shuttle proteins translocating between the cytoplasm and the nucleus (Alt *et al.*, 2005). This could explain why their co-localisation was widely distributed, although MDM2 showed a more speckled appearance both in the nucleus and cytoplasm.

MDM2-NBS1 protein co-localisation was evident in irradiated cells at different time-points post-IR and untreated controls. Although the proteins did not appear to form foci, they seemed to occupy the same subcellular compartments with the same temporal pattern. Further experiments are required involving co-staining for γH2AX and TP53BP2. It would also be beneficial to replicate the results of Alt *et al.,* 2005 in HeLa and 293T cell lines – cancerous and non-cancerous cell lines respectively, both lacking functional p53 and therefore, serving as good models for studying p53-independent functions of MDM2.

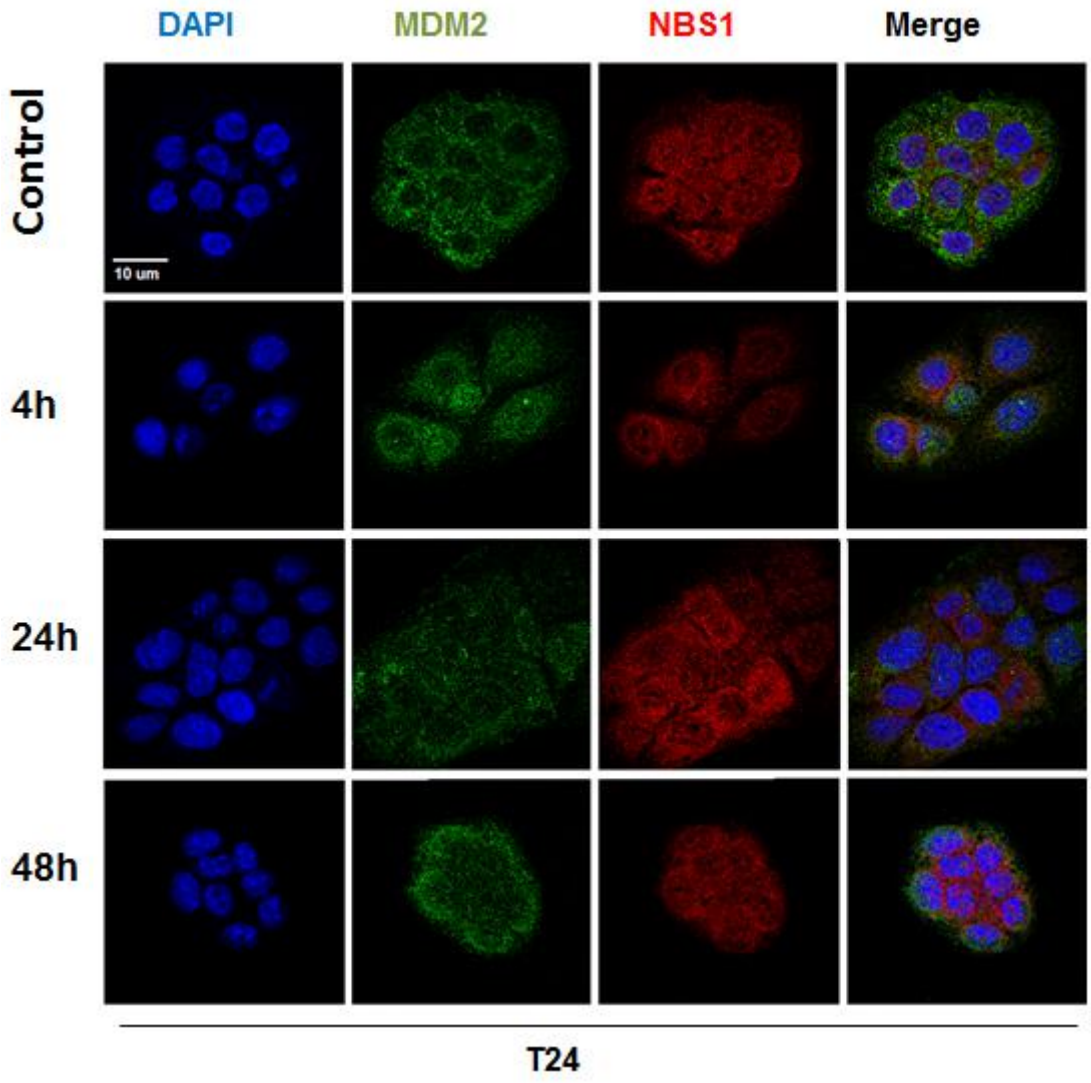

Figure 3.9: Analysis of MDM2 and NBS1 localisation in T24 cells untreated (control) or treated with 5 Gy IR, fixed at 4, 24 and 48 hours post-treatment, stained for NBS1 (red), MDM2 (green) and counterstained with DAPI.

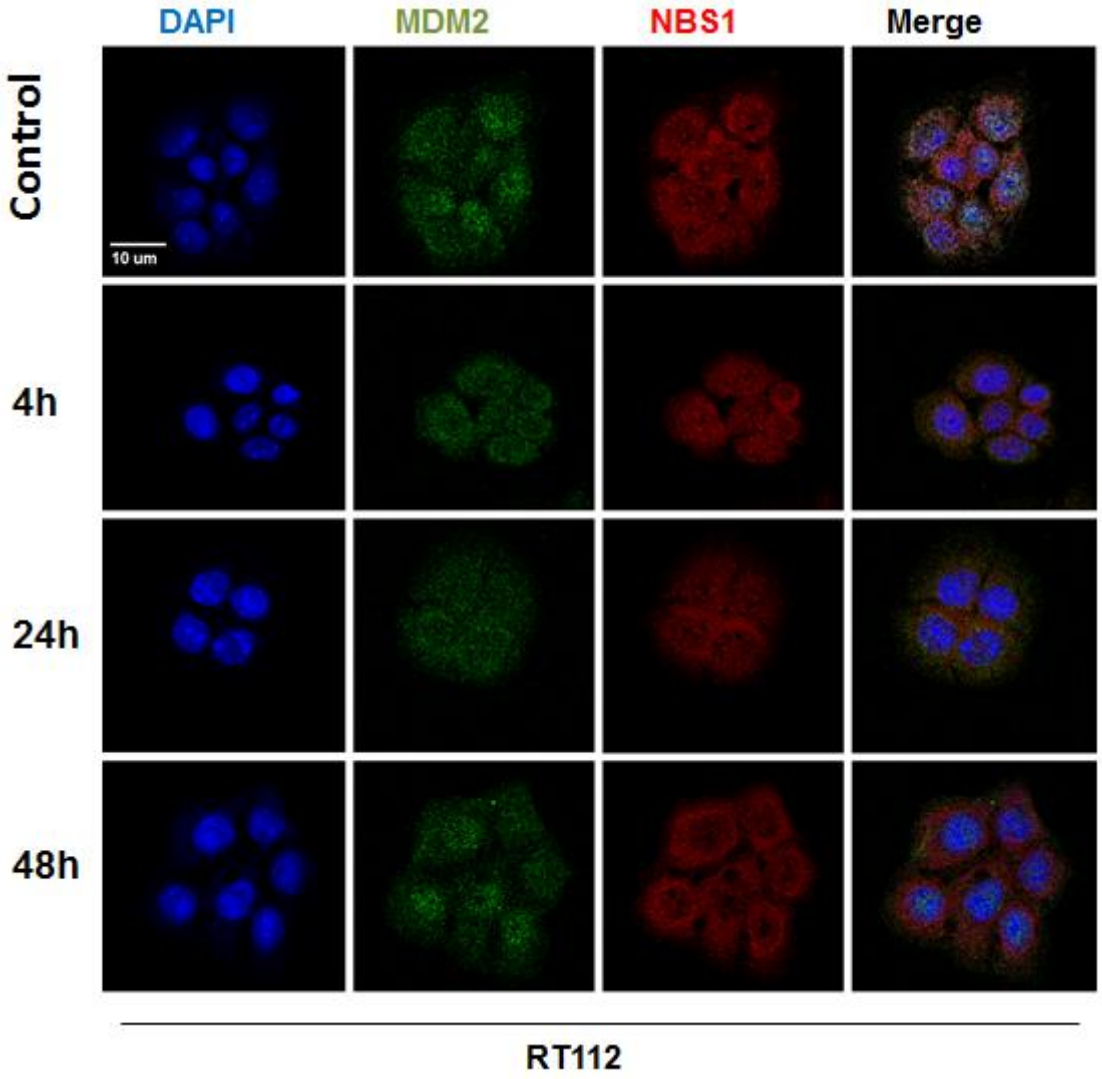

Figure 3.10: Analysis of MDM2 and NBS1 localisation in RT112 cells untreated (control) or treated with 5 Gy IR, fixed at 4, 24 and 48 hours post-treatment, stained for NBS1 (red), MDM2 (green) and counterstained with DAPI.

3.8 NBS1 and MDM2 proteins interact in the absence of genotoxic stress

To determine whether MDM2 and NBS1 interact in unstressed cells, endogenous NBS1 was immunoprecipitated from the whole cell lysates of untreated T24 and RT112 cells. The presence of ~90 kDa protein bands corresponding to MDM2 protein in lanes loaded with NBS1 immunoprecipitated from T24 and RT112 lysates suggests that MDM2 co-immunoprecipitates with NBS1 in both cell lines without treatment. Therefore, in the absence of DNA damage, MDM2 is able to associate with NBS1 (Figure 3.11). The experiment needs to be repeated including the whole cell lysates and protein molecular weight standards.

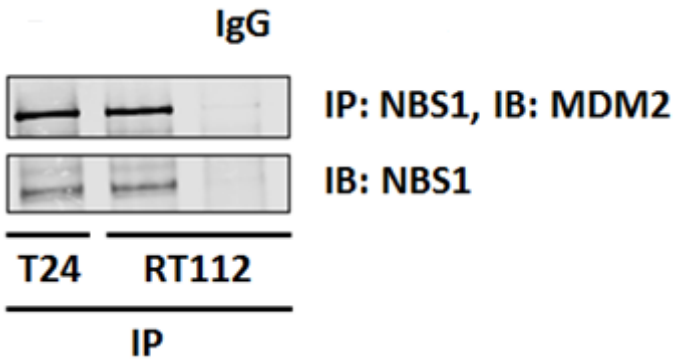

Figure 3.11: Analysis of MDM2-NBS1 protein interaction by co-immunoprecipitation in untreated T24 and RT112 cells. The bands detected by anti-MDM2 [2A10] antibody represent the MDM2-NBS1 protein complex.

3.9 NBS1 is not ubiquitylated in T24 and RT112 cell lines following treatment with 5 Gy IR

In order to test whether NBS1 is ubiquitylated in T24 and RT112 cells and whether it is altered by IR-induced DNA damage, treatment with RG7388, or a combination of RG7388 and IR, endogenous NBS1 was immunoprecipitated (IP) from T24 and RT112 whole cell lysates with an NBS1-specific antibody (IP) and immunoblotted (IB) with anti-conjugated ubiquitin chain antibody, FK2. The FK2 antibody reacts with mono- and polyubiquitylated conjugates, but not with free ubiquitin (Fujimuro *et al.,* 1994; Takada *et al.*, 1997). Following the immunoblotting, FK2 antibody detected no smear of bands in the IP lanes of T24 and RT112, suggesting that NBS1 protein pulled down under the treatment conditions of this study is not modified by ubiquitylation at the chosen time points (Figure 3.12 A-B). Further experiments are required to confirm this result and should include: protein molecular weight standards and positive controls, such as proteins known to be ubiquitylated under these conditions (i.e. immunoprecipitation from the untreated cell lysate following treatment with protease inhibitor MG-132 and/or overexpression of HA-tagged ubiquitin). It would also be beneficial to test other anti-NBS1 and anti-conjugated ubiquitin chain antibodies. A notable smear in the IP fraction of NBS1 from both T24 and RT112 lysates indicates a degradation process or a contaminating signal from other protein. Whether or not the detected signal truly belongs to NBS1 could be confirmed by MS.

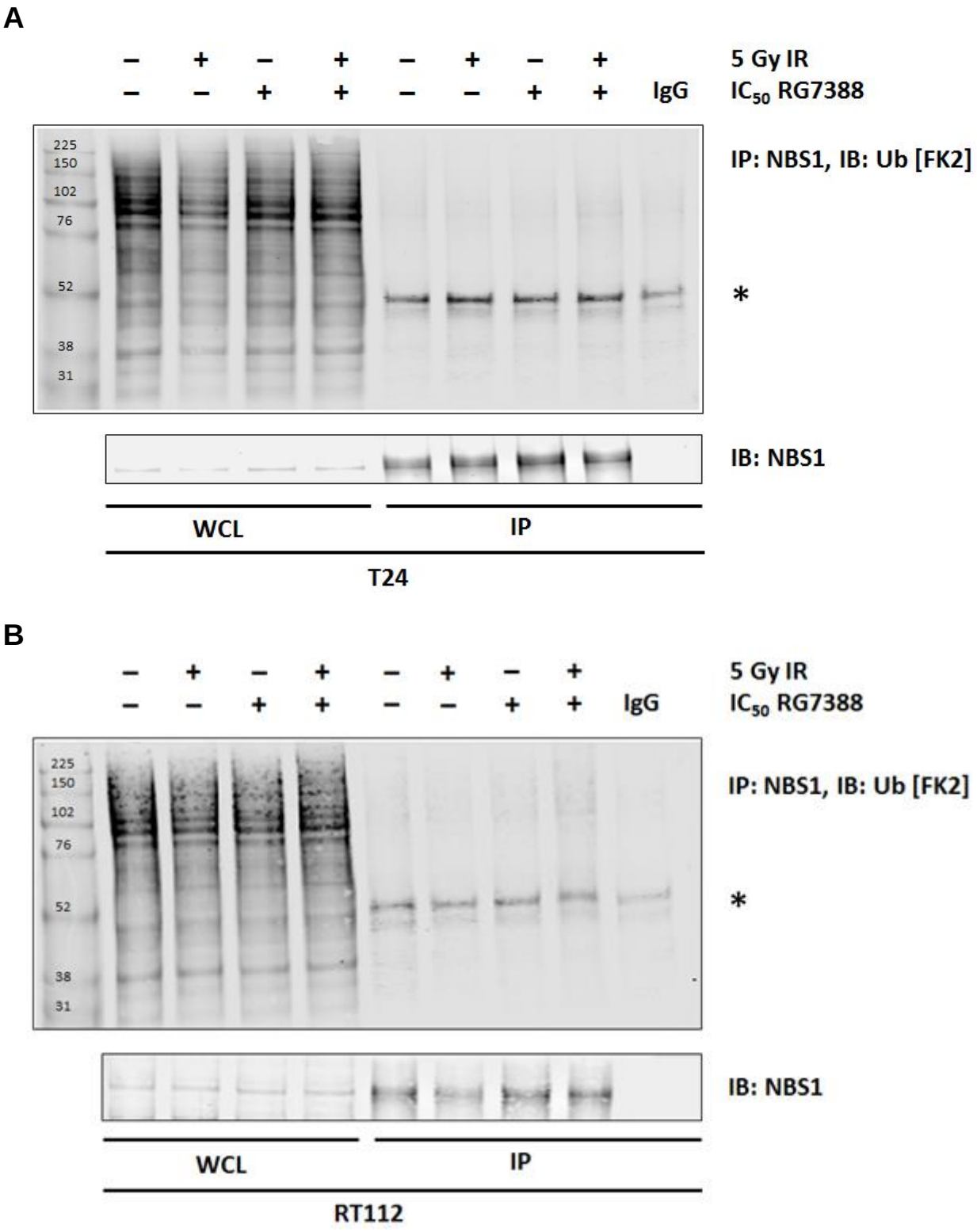

Figure 3.12: Analysis of protein ubiquitylation for NBS1 and binding proteins in A: T24 and B: RT112 cell lines by co-immunoprecipitation following the treatment with IC_{50} dose of RG7388, 5 Gy IR and a combination of the two. * IgG

3.10 RG7388 does not affect the MDM2-NBS1 protein interaction

To determine whether IR-induced DNA damage, treatment with RG7388 or a combination of the two would alter the binding of MDM2 to NBS1, endogenous NBS1 was immunoprecipitated from

T24 and RT112 cells following 24-hour treatment with RG7388 and/or 4 hours after their exposure to 5 Gy IR.

Cells treated with DMSO +/- 5 Gy IR served as negative controls. The immunoprecipitation (IP) was carried out using no antibody (WCL, 300 µg), an isotype control antibody (IgG, 300 µg), or an NBS1-specific antibody (elution, 300 µg). The bands of ~90 kDa detected by immunoblotting with anti-MDM2 [2A10] antibody show that a similar amount of MDM2 co-immunoprecipitated with NBS1 in both cell lines regardless of the treatment (Figure 3.13). Although these results suggest that the MDM2-NBS1 protein interaction is not altered by the IR treatment, whole cell lysates do not always fully reflect changes in protein association if only a fraction of the total protein is involved, nor do whole cell lysates provide information on altered cellular localisation or function of protein complexes.

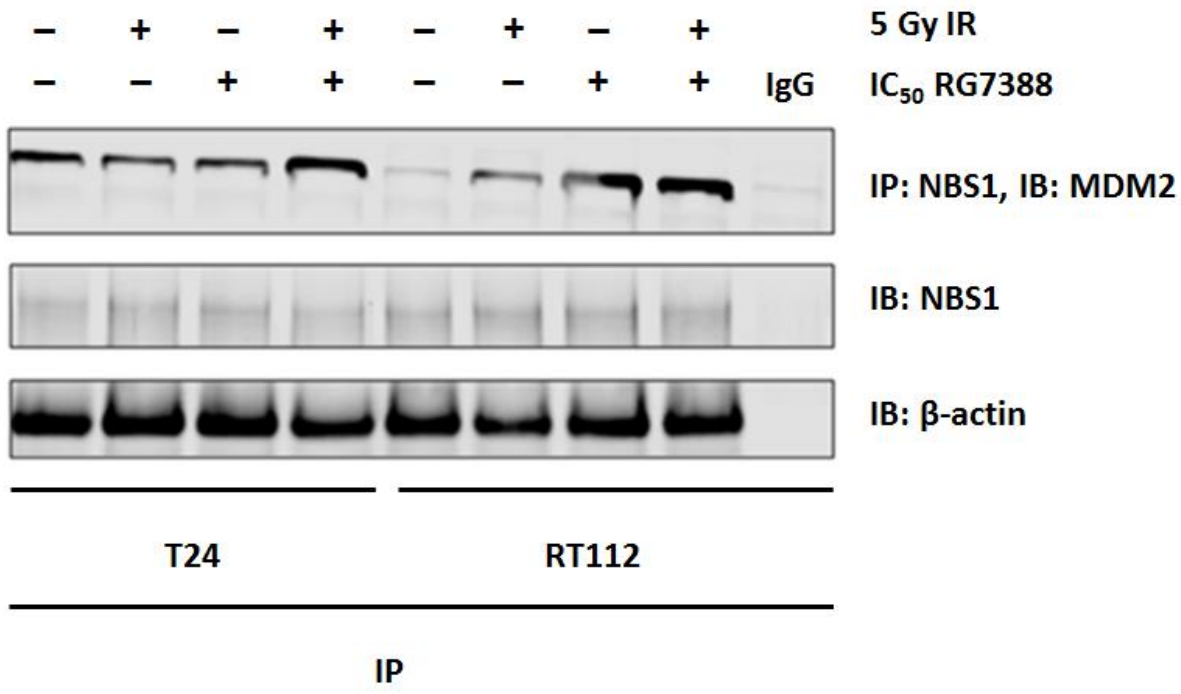

Figure 3.13: Analysis of IC_{50} RG-7388 +/- IR (5Gy) effect on MDM2-NBS1 protein complex by co-immunoprecipitation in T24 and RT112 cell lines. The bands represent the MDM2-NBS1 protein complex band detected by anti-MDM2 [2A10] antibody.

Future experiments should also include the untreated control (i.e. cells treated with DMSO only prior to lysis) and protein molecular weight standards on the WB gel. It is also important to

immunoblot the immunoprecipitated NBS1 for MRE11 and RAD50, which could serve as positive controls for they are known to constitute the MRN complex.

For unclear reasons, we were unable to detect NBS1, MRE11, and RAD50 proteins in immunoprecipitations of endogenous MDM2. Further experiments are required to examine whether co-transfection of HA-tagged NBS1 and FLAG-tagged MDM2 could resolve this issue, resulting in MDM2 protein bands detected in anti-HA immunoprecipitated protein samples. Occasionally the antibody epitopes could be abolished or masked after IP. This issue can be addressed by repeating the experiment with anti-NBS1, -MRE11, -RAD50 and/or –MDM2 antibodies recognizing different epitopes of these proteins. It is also possible that MRE11 and RAD50 are not involved in NBS1-MDM2 interaction. The crystal structure of this protein complex is yet to be solved and may shed light on MRN-independent functions of NBS1.

Chapter 4 Discussion

MDM2 has p53-dependent and independent functions, both of which are likely to contribute to oncogenic and tumour supressing activities (Manfredi, 2010). As a known driving oncogene in 40% of MIBC cases, MDM2 is often a subject to high copy number gain (Cazier *et al.,* 2014; Ganguli and Wasylyk, 2003) (Figure 3.1, Table 3.2). While the MDM2-driven negative regulation of p53 has been thoroughly studied (Meek, 2015), its p53-independent activity is scarcely understood. Overexpression of murine Mdm2, for example, alters DNA ploidy and promotes tumorigenesis independent of p53 expression in mice (Wang *et al.*, 2008), yet the pathways that mediate these MDM2-initiated cellular processes are largely unknown. This project focuses on the identification and characterisation of the protein interaction of MDM2 with the DNA repair protein NBS1 RT112 and T24 cell lines representing different phenotypes of bladder cancer respectively and different mutation status of p53. This project provides new critical insights into the role of this p53-independent protein interaction in DNA repair. As MDM2 is involved in regulating the DNA repair by direct binding to NBS1 of the MRN DNA repair complex in p53-independent manner, it may help to design novel combination therapy strategies to improve the treatment outcomes for cancer patients with p53 mutations.

4.1 RG7388 treatment alone and in combination with IR leads to augmented MDM2 protein levels

As a mediator of genomic instability, MDM2 is upregulated in response to genotoxic stress. Following RG7388 binding to the N-terminal p53 binding site, MDM2 becomes stabilised and can no longer target p53 for proteasomal degradation. However, as p53 expression is regulated by MDM2 via a negative feedback loop, elevated levels of the stabilised p53 will trigger the increase in MDM2 expression. The following experiment series investigating the effect of RG7388 on expression and protein levels of MDM2 and NBS1 focused on two human bladder cancer cell lines

– T24 and RT112. As established earlier by Kiltie group and confirmed by the CNV analysis summarised in this study, they represent luminal and basal bladder cancer phenotypes respectively. Also, T24 cells have a mutant form of p53 while RT112 express a wild type form of this tumour suppressor protein.

Increased mRNA expression of *MDM2* in T24 and RT112 cell lines following their exposure to IR is consistent with previously published results (Figure 3.7 A-B) (Perry *et al.,* 2004). MDM2 serves as a survival factor in many cell types by negatively regulating the apoptotic function of p53. Therefore, IR-induced DNA damage is often followed by elevated mRNA expression of *MDM2*, which in turn shortens the length of the cell cycle arrest established by p53. Elevated protein levels of MDM2 facilitate the return of p53 pro-apoptotic activity to its basal levels in surviving cells (Perry *et al.,* 2004). Additionally, copy number gain of *MDM2* was observed in RT112 cell line (Table 3.2, Appendix 1). This type of copy number alteration event is known to have a positive linear influence on gene expression for the majority of genes. Therefore, it would be interesting to perform a correlation analysis between the copy number and mRNA expression of *MDM2* and *NBN* in RT112 cell line, with observed copy number gain for both of these genes, and contrast it with T24 cell line, where *MDM2* and *NBN* display copy-neutral loss of heterozygosity (cnLOH) events.

Compared to untreated controls, RG7388 but not 5 Gy IR triggered significant elevation of MDM2 protein levels ($p < 0.01$) in both investigated cell lines (Figure 3.8 A-F). The combination treatment with RG7388 and 5 Gy IR also led to markedly augmented MDM2 level compared to untreated controls ($p < 0.01$) and compared to samples treated with 5 Gy IR alone ($p < 0.05$ for T24 and $p < 0.01$ for RT112) (Figure 3.8 A-F). MDM2 upregulation correlates with IR-induced accumulation of p53 (Shi *et al*., 2012). Therefore, the overall difference between T24 and RT112 and the fact that

MDM2 protein levels showed no significant difference compared to untreated controls (p = n.s) are interesting with regard to the p53 status of T24 (mutated p53) and RT112 (wild type p53) cell lines (Hinata *et al.,* 2003). MDM2 has been shown to retain the ability to bind and degrade both wild type and mutant p53. However, the strength of MDM2-p53 protein interaction via DNA binding domain of p53 and transcriptional activation of *MDM2* gene may be severely compromised in p53-mutant cells (Lukashchuk and Vousden, 2007).

mRNA level does not always correspond to protein levels, and one of the reasons for this could be post-translational modifications of the protein in question (Tian *et al.*, 2004; Lundberg *et al.*, 2010; Vogel *et al.*, 2010; Schwanhausser, 2011). Additional limitations for all experiments involving immunoblotting may be imposed by the sensitivity and epitope-binding efficiency of the antibodies chosen for immunoblotting analysis.

The epitope (294-339 aa) recognised by the anti-MDM2 [2A10] antibody lies within exon 9 (GeneTex datasheet, cat # GTX16895), which is one of the most commonly spliced regions of the full length MDM2 transcript (Bartel *et al.*, 2004). Therefore, the protein-coding splice variants of MDM2 lacking the epitope may be undetected. This would diminish the value of the total protein level of MDM2 calculated as a sum of the protein band intensities. The experiments involving immunoblotting could be repeated with a different anti-MDM2 antibody, such as SMP14. The epitope recognised by SMP14 (154-167 aa) is located upstream of the commonly spliced-out sequence region (Abcam datasheet, cat # ab3110). The MDM2 [SMP14] antibody may therefore detect splice variants previously unseen in the western blot experiment. In addition to alternative splicing, the structural, conformational, interactional and functional diversity of protein variants may be further increased by post-translational regulation (Batuello *et al.,* 2015). The post-translational modifications of MDM2 and NBS1 could be analysed by mass spectrometry.

Additional experiments should be undertaken using HeLa and 293T cell lines in order to be able to replicate the experiments by Alt *et al.,* 2005 and confirm the antibody specificity. Neuroendocrine prostate cancer and angiosarcoma cell lines are also of interest for future experiments as they are reported to have the highest expression of MDM2 of all human cancers (Guo *et al.,* 2013; Rayburn *et al.,* 2005). The results of these experiments can then be followed up by ubiquitylation assays that would indicate whether NBS1 is a substrate of E3 ubiquitin ligase MDM2 during the DNA damage response and whether it is mono- or polyubiquitylated. If NBS1 proves to be ubiquitylated by MDM2, MDM2 KD or MDM2 CRISPR KO and/or a cell line expressing a mutant form of MDM2 deficient of NBS1 binding site could serve as negative controls for future experiments and trigger increased protein level of NBS1.

4.2 RG7388 activates the DNA damage response but does not act as a radiosensitiser

Although inhibition of the MDM2-p53 protein interaction by RG7388 and its precursor drugs is reported to have a radiosensitising effect on glioblastoma, lung and prostate cancer (Supiot *et al.,* 2008; Villalonga-Planells *et al.*, 2011; Phelps *et al.*, 2015), this is not the case for T24 and RT112 bladder cancer cell lines with the conditions used in this study.

Compared to untreated control, the number of γH2AX foci in T24 and RT112 cells treated with 5 Gy IR alone and in combination with IC_{50} dose of RG7388 was significantly elevated (Figure 3.3-3.5). However, there was no statistically significant difference in clonogenic survival of cells treated with 0-8 Gy IR vs 0-8 Gy IR in combination with IC_{50} dose of RG7388 (p = n.s) (Figure 3.6 A-B).

Contrary to published studies, the different mutation status of p53 in T24 and RT112 cell lines did not seem to cause significant differences in their radiosensitivity triggered by RG7388. RT112 cells with wild type p53 showed a clonogenic radiosensitivity survival graph similar to that of T24,

harbouring multiple p53-inactivating mutations. The disease-associated mutations of p53 in T24 compared to RT112 cells seem unlikely to affect changes in protein levels of MDM2 and NBS1 following treatment with IC_{50} dose of RG7388, 5 Gy IR or a combination of the two. This supports the hypothesis that p53-independent activity of MDM2 is responsible for regulation of NBS1 protein function in DSB repair.

4.3 NBS1 and MDM2 proteins co-localise in the nucleus and cytoplasm without forming foci

Both NBS1 and MDM2 transcripts are known to contain nuclear localisation signals that allow them to shuttle between the nucleus and cytoplasm. Although the recruitment of NBS1 to sites of DSBs via its interactions with ATM, MDC1 and γH2AX was previously reported to trigger formation of intranuclear foci following DNA damage (Saito, Fujimoto and Kobayashi, 2013), under the same experiment conditions, this was not the case for T24 and RT112 cell lines.

The ability of the wild-type NBS1 and MDM2 proteins to form foci is regulated by the FHA domain (20-108 aa) and RING domain (436-482 aa) respectively. It would be interesting to test whether expression of either the full-length, FHA or RING mutants in cells lacking endogenous NBS1 would reduce the levels of MRN complex proteins in the nucleus and radiosensitise the cells compared to controls expressing wild-type NBN.

NBS1 protein localises predominantly in the nucleus whereas MDM2 is also found in the cytoplasm. By four hours following exposure to 5 Gy IR, cytoplasmic MDM2 protein had translocated from the cytoplasm to the nucleus of T24 and RT112 cells (Figure 3.9-3.10). By twenty-four hours post-irradiation, MDM2 and NBS1 had translocated back to the cytoplasm. NBS1 is known to localise to DSBs as part of the MRN complex during the DNA damage response. However, perhaps following DNA repair, it localises to other parts of the cells, as a part of a

different complex, to perform DNA repair-independent functions. Whether or not this co-occurs with mutations or alternative splicing of FHA or RING sequence regions in NBS1 and MDM2 variants respectively could be validated by a 3'-5' RACE experiment that allows for rapid cDNA end amplification from the full length sequence of the mRNA transcript of the gene of interest. In addition, time points between 0 and 4 hour would be very interesting to look at the dynamics of MDM2 and NBS1 localisation with regards to foci formation directly after induction of DSB.

4.4 Additional experiments are required to establish whether NBS1 is a ubiquitylation substrate of MDM2 RING E3 ligase

It has been reported that the C-terminal ubiquitin ligase domain (198-400 aa) of MDM2 is dispensable for binding to NBS1 delaying DNA repair (Alt *et al.*, 2005). However this does not rule out that NBS1 can be targeted by MDM2 for ubiquitylation (Alt *et al.*, 2005; Bouska *et al.*, 2008; Riley and Lozano, 2012). Accumulating evidence suggests a critical role of NBS1 ubiquitylation in DSB repair. NBS1 serves as a ubiquitylation substrate for multiple proteins involved in different steps of HR, leading to more efficient and precise regulation of DSB repair.

By sequential addition of monomers to its specific lysine or methionine amino acid residues, ubiquitin can form polymer chains of at least eight different linkage types. It is the linkage type of the ubiquitin chain and the target amino acid residue of the substrate protein that determine whether a modified protein is degraded by the proteasome (Lys48-linked polyubiquitin chain) or serves as target to attract binding partner proteins to initiate signalling cascades (Lys6-, Lys11-, Lys27-, Lys29-, Lys33-, Lys63-, and Met1-linked mono- and polyubiquitin). The ubiquitylation activity of RNF8, for example, contributes to efficient recruitment and stable association of NBS1 with chromatin containing DSBs and promotes HR-mediated DNA repair (Huen *et al.*, 2007; Lu *et*

al., 2012). It is also known that NBS1 is ubiquitylated by SKP2 to stimulate ATM-initiated activation of the DNA damage checkpoint (Wu *et al.*, 2012).

The co-immunoprecipitation of MDM2 and NBS1 from T24 and RT112 cells treated with 5 Gy IR, IC_{50} dose of RG-7388 and a combination of the two showed that the two proteins interact before and after DNA damage (Figure 3.11, 3.13). However, the experiment should be repeated with additional controls, such as whole cell lysates and protein molecular weight standards. Immunoprecipitation and immunoblotting experiments should be undertaken using the antibodies specific for different epitopes of MDM2 to address the potential antibody specificity problem. As suggested in Section 4.1., additional negative controls such as MDM2 KO or KD, MDM2 mutant lacking NBS1 binding site and/or functional RING domain, all of which could potentially result in NBS1 build-up, are crucial to facilitate our understanding of the MDM2-NBS1 interaction and ways of its regulation.

The same phenomenon has been reported for NBS1-RNF8 protein interaction, which is known to stabilize the interaction of NBS1 with DSBs (Lu et al., 2012). This raises the question whether MDM2 may be modulating NBS1 association with DSBs in cooperation with other E3 ligases.

A western blot has been performed to determine whether NBS1 was ubiquitylated, in T24 and RT112 cells lines (Figure 3.12). Anti-conjugated ubiquitin chain (FK2) antibody detected no ubiquitylation-specific smears in the immunoprecipitations of NBS1 from T24 and RT112 lysates. This suggests that following treatment with 5 Gy IR, the IC_{50} dose of RG-7388, or a combination of the two, NBS1 is not ubiquitylated in either of investigated cell lines.

Ubiquitylation is a dynamic process (Schwertman *et al.,* 2016). Therefore, repeating this experiment with a wider range of time points following the same treatment regimens would shed light on whether NBS1 is instead ubiquitylated before or after the four-hour time point. It is also possible that ubiquitylation sites in NBS1 are affected by alternative splicing or disease-associated mutations of *NBN* and *MDM2* in T24 and RT112 cell lines. Additional co-immunoprecipitation and mass spectrometry analysis is required to verify whether NBS1 is ubiquitylated. If it is, co-immunoprecipitation assays can be undertaken for cells treated with MG-132 proteasome inhibitor in order to determine whether ubiquitulation regulates the NBS1 protein levels by proteasomal degradation or its protein-protein interactions and signalling.

In conclusion, we demonstrated that the selective small-molecule inhibitor of MDM2, RG7388, induces the DNA damage response but does not enhance the radiosensitivity of T24 and RT112 bladder cancer cell lines by inhibition of MDM2. Consistent with published studies, RG7388 treatment results in increased protein levels of MDM2 by directly binding to and stabilising its N-terminal hydrophobic p53 binding pocket. This, in turn, promotes the p53- and ubiquitylation-independent protein interaction between MDM2 and NBS1 that is reported to delay DNA double-strand break repair and prolong DNA damage response signaling. The mechanism of how MDM2 regulates NBS1 function remains elusive. Future experiments could include the mass spectrometry analysis of post-translational modifications that may be involved in regulation of the MDM2-NBS1 complex assembly, and more experiments examining the dynamics of subcellular localisation of NBS1 and MDM2 and their impact on DDR.

Conclusions

- The CNA analysis confirmed that RT112 and T24 cell lines represent luminal and basal phenotypes of bladder cancer respectively.
- RT112 cell line demonstrated copy number gain of both MDM2 and NBN genes, unlike T24 cell line, where both genes had copy-neutral loss of heterozygocity.
- RG7388 and IR treatment resulted in elevated mRNA expression and protein levels of MDM2.
- Following 5 Gy IR treatment of T24 and RT112 cells, NBS1 and MDM2 co-localised without foci formation.
- As shown in pilot IP experiment, NBS1 and MDM2 proteins could interact in the absence of genotoxic stress.
- NBS1 did not appear ubiquitylated in T24 and RT112 cell lines following treatment with 5 Gy IR.
- RG7388 treatment did not affect the MDM2-NBS1 protein interaction.

Future Work

- Linear correlation analysis of *MDM2* and *NBN* copy number alteration events and mRNA expression levels in RT112 and T24.
- Negative controls such as MDM2 CRISPR KO or KD cell line or MDM2 with point mutation(s) blocking its interaction with NBS1 and/or inhibiting its E3 ligase activity.
- Cyclohexamide treatment in order to be able to inhibit the protein synthesis and determine the half-life of MDM2 and NBS1.
- IF experiments to include co-staining for γH2AX and TP53BP2.

- Prior to troubleshooting it in RT112 and T24 cells, replicate the IF and IP results of Alt *et al.,* 2005 in HeLa and 293T cell lines – cancerous and non-cancerous cell lines respectively, both lacking functional p53 and therefore, serving as good models for studying p53-independent functions of MDM2.
- All immunoprecipitation experiments to include protein molecular weight standards, whole cell lysates, loading controls, positive and negative controls.
- Experiment involving NBS1 immunoprecipitated (IP) from T24 and RT112 whole cell lysates with an NBS1-specific antibody (IP) and immunoblotted (IB) with anti-conjugated ubiquitin chain antibody, FK2 should be repeated with additional positive controls. Immunoprecipitated NBS1 should be immunoblotted for MRE11 and RAD50, as positive controls for they are known to constitute the MRN complex.
- Mass spectrometry analysis of immunoprecipitated NBS1 would help us gain a better insight of its binding partners and post-translational modifications under different treatment conditions.

References

Van Allen, E. M., Mouw, K. W., Kim, P., Iyer, G., Wagle, N., Al-Ahmadie, H., Zhu, C., Ostrovnaya, I., Kryukov, G. V., O'connor, K. W., Sfakianos, J., Garcia-Grossman, I., Kim, J., Guancial, E. A., Bambury, R., Bahl, S., Gupta, N., Farlow, D., Qu, A., Signoretti, S., Barletta, J. A., Reuter, V., Boehm, J., Lawrence, M., Getz, G., Kantoff, P., Bochner, B. H., Choueiri, T. K., Bajorin, D. F., Solit, D. B., Gabriel, S., D'andrea, A., Garraway, L. A. and Rosenberg, J. E. (2014) 'Somatic ERCC2 mutations correlate with cisplatin sensitivity in muscle-invasive urothelial carcinoma', *Cancer Discovery*, 4(10), pp. 1140–1153. doi: 10.1158/2159-8290.CD-14-0623.

Alt, J. R., Bouska, A., Fernandez, M. R., Cerny, R. L., Xiao, H. and Eischen, C. M. (2005) 'Mdm2 binds to Nbs1 at sites of DNA damage and regulates double strand break repair', *Journal of Biological Chemistry*, 280(19), pp. 18771–18781. doi: 10.1074/jbc.M413387200.

Antoni, S., Ferlay, J., Soerjomataram, I., Znaor, A., Jemal, A. and Bray, F. (2017). Bladder Cancer Incidence and Mortality: A Global Overview and Recent Trends. *European Urology*, 71(1), pp.96-108.

Asahara, H., Li, Y., Fuss, J., Haines, D. S., Vlatkovic, N., Boyd, M. T. and Linn, S. (2003) 'Stimulation of human DNA polymerase epsilon by MDM2', *Nucleic acids research*, 31(9), pp. 2451–9. doi: 10.1093/nar/gkg342.

Ayers, S. D., Nedrow, K. L., Gillilan, R. E. and Noy, N. (2007) 'Continuous nucleocytoplasmic shuttling underlies transcriptional activation of PPARgamma by FABP4', *Biochemistry*, 46(23), pp. 6744–6752. doi: 10.1021/bi700047a.

Bartel, F., Harris, L. C., Würl, P. and Taubert, H. (2004) 'MDM2 and Its Splice Variant Messenger RNAs : Expression in Tumors and Down-Regulation Using Antisense Oligonucleotides 1 1 NIH grants CA92401 and CA21765 , American Lebanese Syrian Associated Charities (L .C.H .), MDM2 and Its Splice Variant Messenger', *Molecular cancer Research*, 2, pp. 29–35.

Batuello, C. N., Hauck, P. M., Gendron, J. M., Lehman, J. A. and Mayo, L. D. (2015) 'Src phosphorylation converts Mdm2 from a ubiquitinating to a neddylating E3 ligase', Proceedings of the National Academy of Sciences of the United States of America, 112(6), pp. 1749–54. doi: 10.1073/pnas.1416656112.

Bentley, J., Diggle, C. P., Harnden, P., Knowles, M. A. and Kiltie, A. E. (2004) 'DNA double strand break repair in human bladder cancer is error prone and involves microhomology-associated end-joining', *Nucleic Acids Research*, 32(17), pp. 5249–5259. doi: 10.1093/nar/gkh842.

Bouska, A., Lushnikova, T., Plaza, S. and Eischen, C. M. (2008) 'Mdm2 promotes genetic instability and transformation independent of p53', *Molecular and cellular biology*, 28(15), pp. 4862–4874. doi: 10.1128/MCB.01584-07.

Bouska A, Eischen C. (2009) Mdm2 Affects Genome Stability Independent of p53. *Cancer Research,* 69(5), pp. 1697-1701.

Bubenik J, Baresova M, Viklicky V, Jakoubkova J, Sainerova H, D. J. (1973) 'Established cell line of urinary bladder carcinoma (T24) containing tumour-specific antigen', *International Journal of Cancer*, 11, pp. 765–773.

Bueren-Calabuig, J. A. and Michel, J. (2016) 'Impact of Ser17 phosphorylation on the

conformational dynamics of the oncoprotein MDM2', *Biochemistry*, 55(17), pp. 2500–2509. doi: 10.1021/acs.biochem.6b00127.

Candeias, M. M., Malbert-Colas, L., Powell, D. J., Daskalogianni, C., Maslon, M. M., Naski, N., Bourougaa, K., Calvo, F. and Fåhraeus, R. (2008) 'P53 mRNA controls p53 activity by managing Mdm2 functions', *Nature cell biology*, 10(9), pp. 1098–105. doi: 10.1038/ncb1770.

Carrillo, A. M., Bouska, A., Arrate, M. P. and Eischen, C. M. (2015) 'Mdmx promotes genomic instability independent of p53 and Mdm2', *Oncogene*, 34(7), pp. 846–856. doi: 10.1038/onc.2014.27.Mdmx.

Carter, S., Bischof, O., Dejean, A. and Vousden, K. (2007). C-terminal modifications regulate MDM2 dissociation and nuclear export of p53. *Nature Cell Biology*, 9(4), pp.428-435.

Cazier, J.-B., Rao, S. R., McLean, C. M., Walker, a L., Wright, B. J., Jaeger, E. E. M., Kartsonaki, C., Marsden, L., Yau, C., Camps, C., Kaisaki, P., Taylor, J., Catto, J. W., Tomlinson, I. P. M., Kiltie, a E. and Hamdy, F. C. (2014) 'Whole-genome sequencing of bladder cancers reveals somatic CDKN1A mutations and clinicopathological associations with mutation burden', *Nature communications*, 5, p. 3756. doi: 10.1038/ncomms4756.

Choi, W., Porten, S., Kim, S., Willis, D., Plimack, E. R., Roth, B., Cheng, T., Tran, M., Lee, I., Melquist, J., Bondaruk, J., Majewski, T., Zhang, S., Pretzsch, S. and Baggerly, K. (2014) 'Identification of distinct basal and luminal subtypes of muscle-invasive bladder cancer with different sensitivities to frontline chemotherapy', *Cancer Cell,* 25(2), pp. 152–165. doi: 10.1016/j.ccr.2014.01.009.Identification.

Conradt, L., Henrich, A., Wirth, M., Reichert, M., Lesina, M., Algül, H., Schmid, R. M., Krämer, O. H., Saur, D. and Schneider, G. (2013) 'Mdm2 inhibitors synergize with topoisomerase II inhibitors to induce p53-independent pancreatic cancer cell death', *International journal of cancer. Journal international du cancer*, 132(10), pp. 2248–57. doi: 10.1002/ijc.27916.

Cordon-Cardo C, Latres E, Drobnjak M, et al. Molecular abnormalities of mdm2 and p53 genes in adult soft tissue sarcomas. (1994) *Cancer Res,* 54(3), pp. 794-799.

Dadhania, V., Zhang, M., Zhang, L., Bondaruk, J., Majewski, T., Siefker-Radtke, A., Guo, C., Dinney, C., Cogdell, D., Zhang, S., Lee, S., Lee, J., Weinstein, J., Baggerly, K., McConkey, D. and Czerniak, B. (2016). Meta-Analysis of the Luminal and Basal Subtypes of Bladder Cancer and the Identification of Signature Immunohistochemical Markers for Clinical Use. *EBioMedicine*, 12, pp.105-117.

Dastidar, S. G., Raghunathan, D., Nicholson, J., Hupp, T. R., Lane, D. P. and Verma, C. S. (2011) 'Chemical states of the N-terminal "lid" of MDM2 regulate p53 binding: Simulations reveal complexities of modulation', *Cell Cycle*, 10(1), pp. 82–89. doi: 10.4161/cc.10.1.14345.

Deisenroth, C. and Zhang, Y. (2010) 'Ribosome biogenesis surveillance: probing the ribosomal protein-Mdm2-p53 pathway', *Oncogene*, 29(30), pp. 4253–4260. doi: 10.1038/onc.2010.189.

Deriano, L., Stracker, T. H., Baker, A., Petrini, J. H. J. and B, D. (2010) 'J recombination intermediates', *Molecular Biology*, 34(1), pp. 13–25. doi: 10.1016/j.molcel.2009.03.009.Roles.

Desai-Mehta, A., Cerosaletti, K. M. and Concannon, P. (2001) 'Distinct Functional Domains of Nibrin Mediate Mre11 Binding , Focus Formation , and Nuclear Localization Distinct Functional Domains of Nibrin Mediate Mre11 Binding , Focus Formation , and Nuclear Localization',

Molecular and Cellular Biology, 21(6), pp. 2184–2191. doi: 10.1128/MCB.21.6.2184.

Ding, Q., Zhang, Z., Liu, J., Jiang, N., Zhang, J., Ross, T. M., Chu, X., Bartkovitz, D., Podlaski, F., Janson, C., Tovar, C., Filipovic, Z. M., Higgins, B., Glenn, K., Packman, K., Vassilev, L. T. and Graves, B. (2013) 'Discovery of RG7388, a Potent and Selective p53 − MDM2 Inhibitor in Clinical Development', *Journal of Medicinal Chemistry,* 56 (14), pp. 5979–5983.

Elliott, A. Y., Bronson, D. L., Cervenka, J., Stein, N. and Fraley, E. E. (1977) 'Properties of cell lines established from transitional cell cancers of the human urinary tract.', *Cancer research*, 37(5), pp. 1279–1289.

EL-Meghawry EL-Kenawy A, EL-kott A, Khalil A. (2003) Prognostic value of p53 and MDM2 expression in bilharziasis-associated squamous cell carcinoma of the urinary bladder. *The International Journal of Biological Markers,* 18(4), pp. 284-289.

El-Taji, O., Alam, S. and Hussain, S. (2016). Bladder Sparing Approaches for Muscle-Invasive Bladder Cancers. *Current Treatment Options in Oncology*, 17(3).

Fåhraeus, R. and Olivares-Illana, V. (2014) 'MDM2's social network', *Oncogene*, 33(35), pp. 4365–4376. doi: 10.1038/onc.2013.410.

Farina, M., Lundgren, K. and Bellmunt, J. (2017). Immunotherapy in Urothelial Cancer: Recent Results and Future Perspectives. *Drugs*, 77(10), pp.1077-1089.

Feeley K, Adams C, Mitra R, Eischen C. (2017) Mdm2 Is Required for Survival and Growth of p53-Deficient Cancer Cells. *Cancer Research*, 77(14), pp. 3823-3833.

Fogh, J., Fogh, J. M. and Orfeo, T. (1977) 'One hundred and twenty-seven cultured human tumor cell lines producing tumors in nude mice', *JNCI Cancer Spectrum*, 59(1), pp. 221–226.

Freeman J. Copy number variation: New insights in genome diversity. (2006) *Genome Research*, 16(8), pp. 949-961.

Fujimuro, M., Sawada, H. and Yokosawa, H. (1994) 'Production and characterization of monoclonal antibodies specific to multi-ubiquitin chains of polyubiquitinated proteins', *FEBS Letters*, 349(2), pp. 173–180. doi: 10.1016/0014-5793(94)00647-4.

Ganguli, G. and Wasylyk, B. (2003) 'p53-independent functions of MDM2', *Molecular Cancer Research,* 1(14), pp. 1027-1035.

Grossman HB, Wedemeyer G, Ren L, Wilson GN, C. B. (1986) 'Improved growth of human urothelial carcinoma cell cultures', *The Journal of urology*, 136(4), pp. 953–959.

Guo, G., Sun, X., Chen, C., Wu, S., Huang, P., Li, Z., Dean, M., Huang, Y., Jia, W., Zhou, Q., Tang, A., Yang, Z., Li, X., Song, P., Zhao, X., Ye, R., Zhang, S., Lin, Z., Qi, M., Wan, S., Xie, L., Fan, F., Nickerson, M. L., Zou, X., Hu, X., Xing, L., Lv, Z., Mei, H., Gao, S., Liang, C., Gao, Z., Lu, J., Yu, Y., Liu, C., Li, L., Fang, X., Jiang, Z., Yang, J., Li, C., Zhao, X., Chen, J., Zhang, F., Lai, Y., Lin, Z., Zhou, F., Chen, H., Chan, H. C., Tsang, S., Theodorescu, D., Li, Y., Zhang, X., Wang, J., Yang, H., Gui, Y., Wang, J. and Cai, Z. (2013) 'Whole-genome and whole-exome sequencing of bladder cancer identifies frequent alterations in genes involved in sister chromatid cohesion and segregation', *Nature genetics*, 45(12), pp. 1459–63. doi: 10.1038/ng.2798.

Hamzehloie, T., Mojarrad, M., Hasanzadeh-Nazarabadi, M. and Shekouhi, S. (2012) 'The role of

tumor protein 53 mutations in common human cancers and targeting the murine double minute 2-P53 interaction for cancer therapy', *Iranian Journal of Medical Sciences*, 37(1), pp. 3–8.

Hanahan, D. and Weinberg, R. A. (2000) 'The hallmarks of cancer', *Cell*, 100(1), pp. 57–70. doi: 10.1007/s00262-010-0968-0.

Hanahan, D. and Weinberg, R. A. (2011) 'Hallmarks of cancer: The next generation', *Cell*, 144(5), pp. 646–674. doi: 10.1016/j.cell.2011.02.013.

Hinata, N., Shirakawa, T., Zhang, Z., Matsumoto, A., Fujisawa, M., Okada, H., Kamidono, S., Gotoh, A. (2003) 'Radiation induces p53-dependent cell apoptosis in bladder cancer cells with wild-type-p53 but not in p53-mutated bladder cancer cells', *Urological Research,* 31(6), pp. 387-396.

Honda, R., Tanaka, H. and Yasuda, H. (1997) 'Oncoprotein MDM2 is a ubiquitin ligase E3 for tumor suppressor p53', *FEBS Letters*, 420(1), pp. 25–27. doi: 10.1016/S0014-5793(97)01480-4.

Hubbard, T., Barker, D., Birney, E., Cameron, G., Chen, Y., Clark, L., Cox, T., Cuff, J., Curwen, V., Down, T., Durbin, R., Eyras, E., Gilbert, J., Hammond, M., Huminiecki, L., Kasprzyk, A., Lehvaslaiho, H., Lijnzaad, P., Melsopp, C., Mongin, E., Pettett, R., Pocock, M., Potter, S., Rust, A., Schmidt, E., Searle, S., Slater, G., Smith, J., Spooner, W., Stabenau, A., Stalker, J., Stupka, E., Ureta-Vidal, A., Vastrik, I. and Clamp, M. (2002) 'The Ensembl genome database project', *Nucleic acids research*, 30(1), pp. 38–41. doi: 10.1093/NAR/30.1.38.

Huen, M. S., Grant, R., Manke, I., Minn, K., Yu, X., Yaffe, M. B. and Chen, J. (2007) 'The E3 ubiquitin ligase RNF8 transduces the DNA damage signal via an ubiquitin-dependent signaling pathway', *Cell*, 131(5), pp. 901–914. doi: 10.3816/CLM.2009.n.003.Novel.

Ioachim E, Charchanti A, Stavropoulos NE, Skopelitou A, Athanassiou ED, Agnantis NJ. Immunohistochemical expression of retinoblastoma gene product (Rb), p53 protein, MDM2, c-erbB-2, HLA-DR and proliferation indices in human urinary bladder carcinoma. Histol Histopathol. 2000;15(3):721-727. doi:10.14670/HH-15.721

Itahana, K., Mao, H., Jin, A., Itahana, Y., Clegg, H., Lindström, M., Bhat, K., Godfrey, V., Evan, G. and Zhang, Y. (2007). Targeted Inactivation of Mdm2 RING Finger E3 Ubiquitin Ligase Activity in the Mouse Reveals Mechanistic Insights into p53 Regulation. *Cancer Cell*, 12(4), pp.355-366.

Jones S, Hancock A, Vogel H, Donehower L, Bradley A. (1998) Overexpression of Mdm2 in mice reveals a p53-independent role for Mdm2 in tumorigenesis. *Proceedings of the National Academy of Sciences,* 95(26), pp. 15608-15612.

Kamat, A. M., Hahn, N. M., Efstathiou, J. A., Lerner, S. P., Malmstr??m, P. U., Choi, W., Guo, C. C., Lotan, Y. and Kassouf, W. (2016) 'Bladder cancer', *The Lancet*, 388. doi: 10.1016/S0140-6736(16)30512-8.

Karni-Schmidt, O., Castillo-Martin, M., HuaiShen, T., Gladoun, N., Domingo-Domenech, J., Sanchez-Carbayo, M., Li, Y., Lowe, S., Prives, C. and Cordon-Cardo, C. (2011) 'Distinct expression profiles of p63 variants during urothelial development and bladder cancer progression', *American Journal of Pathology*, 178(3), pp. 1350–1360. doi: 10.1016/j.ajpath.2010.11.061.

Kato, S., Goodman, A. M., Walavalkar, V., Barkauskas, D. A., Sharabi, A. and Kurzrock, R. (2017) 'Hyper-progressors after Immunotherapy: Analysis of Genomic Alterations Associated with Accelerated Growth Rate', *Clinical Cancer Research*, p. clincanres.3133.2016. doi: 10.1158/1078-0432.CCR-16-3133.

Kato S, Ross J, Gay L, Dayyani F, Roszik J, Subbiah V et al. (2018) Analysis of MDM2 Amplification: Next-Generation Sequencing of Patients With Diverse Malignancies. JCO *Precision Oncology,* 2, pp. 1-14.

Kawai, K., Miyazaki, J., Joraku, A., Nishiyama, H. and Akaza, H. (2013) 'Bacillus Calmette-Guerin (BCG) immunotherapy for bladder cancer: Current understanding and perspectives on engineered BCG vaccine', *Cancer Science*, 104(1), pp. 22–27. doi: 10.1111/cas.12075.

Kim, P. H., Cha, E. K., Sfakianos, J. P., Iyer, G., Zabor, E. C., Scott, S. N., Ostrovnaya, I., Ramirez, R., Sun, A., Shah, R., Yee, A. M., Reuter, V. E., Bajorin, D. F., Rosenberg, J. E., Schultz, N., Berger, M. F., Al-Ahmadie, H. A., Solit, D. B. and Bochner, B. H. (2015) 'HHS Public Access', *European Urology*, 21(18), pp. 4062–4072. doi: 10.1158/1078-0432.CCR-15-0428.Bioactivity.

Kim, S. P., Frank, I., Cheville, J. C., Thompson, R. H., Weight, C. J., Thapa, P. and Boorjian, S. A. (2012) 'The impact of squamous and glandular differentiation on survival after radical cystectomy for urothelial carcinoma', *Journal of Urology*, 188(2), pp. 405–409. doi: 10.1016/j.juro.2012.04.020.

Knowles, M. A. and Hurst, C. D. (2015) 'Molecular biology of bladder cancer: new insights into pathogenesis and clinical diversity', *Nature Reviews Cancer*, 15(1), pp. 25–41. doi: 10.1038/nrc3817.

Kobayashi, J., Tauchi, H., Sakamoto, S., Nakamura, A., Morishima, K. ichi, Matsuura, S., Kobayashi, T., Tamai, K., Tanimoto, K. and Komatsu, K. (2002) 'NBS1 localizes to γ-H2AX foci through interaction with the FHA/BRCT domain', *Current Biology*, 12(21), pp. 1846–1851. doi: 10.1016/S0960-9822(02)01259-9.

Kruse, J. and Gu, W. (2009). Modes of p53 Regulation. *Cell*, 137(4), pp.609-622.

Kuo, L. J. and Yang, L.-X. (2008) 'Gamma-H2AX - a novel biomarker for DNA double-strand breaks', *In vivo*, 22(3), pp. 305–9. doi: 0258-851X/2008.

Kussie, P. H., Gorina, S., Marechal, V., Elenbaas, B., Moreau, J., Levine, a J. and Pavletich, N. P. (1996) 'Structure of the MDM2 oncoprotein bound to the p53 tumor suppressor transactivation domain', *Science*, 274(5289), pp. 948–953. doi: 10.1126/science.274.5289.948.

Lee J. (2005) ATM Activation by DNA Double-Strand Breaks Through the Mre11-Rad50-Nbs1 Complex. *Science,* 308(5721), pp. 551-554.

Levine, a J., Hu, W. and Feng, Z. (2006) 'The P53 pathway: what questions remain to be explored?', *Cell death and differentiation*, 13(6), pp. 1027–1036. doi: 10.1038/sj.cdd.4401910.

Lu ML, Wikman F, Orntoft TF, et al. Impact of alterations affecting the p53 pathway in bladder cancer on clinical outcome, assessed by conventional and array-based methods. Clin Cancer Res. 2002;8(1):171-179.

Lu, C. S., Truong, L. N., Aslanian, A., Shi, L. Z., Li, Y., Hwang, P. Y. H., Koh, K. H., Hunter, T., Yates, J. R., Berns, M. W. and Wu, X. (2012) 'The RING finger protein RNF8 ubiquitinates Nbs1 to promote DNA double-strand break repair by homologous recombination', *Journal of Biological Chemistry*, 287(52), pp. 43984–43994. doi: 10.1074/jbc.M112.421545.

Lukashchuk, N. and Vousden, K.H. (2007) 'Ubiquitination and degradation of mutant p53', *Molecular and Cellular Biology,* 27(23), pp. 8284-8295.

Lundberg, E., Fagerberg, L., Klevebring, D., Matic, I., Geiger, T., Cox, J., Algenäs, C., Lundeberg, J., Mann, M. and Uhlen, M. (2010) 'Defining the transcriptome and proteome in three functionally different human cell lines.', *Molecular systems biology*, 6(450), p. 450. doi: 10.1038/msb.2010.106.

Lushnikova, T., Bouska, A., Odvody, J., Dupont, W. D. and Eischen, C. M. (2016) 'HHS Public Access', *Oncogene*, 8(5), pp. 583–592. doi: 10.1002/aur.1474.Replication.

Ma, J., Martin, J. D., Zhang, H., Auger, K. R., Ho, T. F., Kirkpatrick, R. B., Grooms, M. H., Johanson, K. O., Tummino, P. J., Copeland, R. A. and Lai, Z. (2006) 'A second p53 binding site in the central domain of Mdm2 is essential for p53 ubiquitylation', *Biochemistry*, 45(30), pp. 9238–9245. doi: 10.1021/bi060661u.

MacDonald, J. R., Ziman, R., Yuen, R. K. C., Feuk, L. and Scherer, S. W. (2014) 'The Database of Genomic Variants: A curated collection of structural variation in the human genome', *Nucleic Acids Research*, 42(D1), pp. 986–992. doi: 10.1093/nar/gkt958.

Manfredi, J. J. (2010) 'The Mdm2-p53 relationship evolves: Mdm2 swings both ways as an oncogene and a tumor suppressor', Genes & Development, 24(15), pp. 1580-1589. doi: 10.1101/gad.1941710.priate.

Marine, J., Francoz, S., Maetens, M., Wahl, G., Toledo, F. and Lozano, G. (2006). Keeping p53 in check: essential and synergistic functions of Mdm2 and Mdm4. *Cell Death & Differentiation*, 13(6), pp.927-934.

Masters, J. R., Hepburn, P. J., Walker, L., Highman, W. J., Trejdosiewicz, L. K., Povey, S., Parkar, M., Hill, B. T., Riddle, P. R. and Franks, L. M. (1986) 'Tissue culture model of transitional cell carcinoma: characterization of twenty-two human urothelial cell lines', *Cancer research*, 46(7), pp. 3630–6.

McDonnell T, Montes de Oca Luna R, Cho S, Amelse L, Chavez-Reyes A, Lozano G. (1999) Loss of one but not twomdm2 null alleles alters the tumour spectrum inp53 null mice. *The Journal of Pathology*, 188(3), pp. 322-328.

Meek, D. W. (2015) 'Regulation of the p53 response and its relationship to cancer', *The Biochemical journal*, 469(3), pp. 325–46. doi: 10.1042/BJ20150517.

Mendoza M, Mandani G, Momand J. (2014) The MDM2 gene family. *BioMolecular Concepts*, 5(1), pp. 9-19.

Migliorini D, Danovi D, Colombo E, Carbone R, Pelicci P, Marine J. (2001) Hdmx Recruitment into the Nucleus by Hdm2 Is Essential for Its Ability to Regulate p53 Stability and Transactivation. *Journal of Biological Chemistry,* 277(9), pp. 7318-7323.

Mitra, A. P., Bartsch, C. C., Bartsch, G., Miranda, G., Skinner, E. C. and Daneshmand, S. (2014) 'Does presence of squamous and glandular differentiation in urothelial carcinoma of the bladder at cystectomy portend poor prognosis? An intensive case-control analysis', *Urologic Oncology: Seminars and Original Investigations*, 32(2), pp. 117–127. doi: 10.1016/j.urolonc.2012.08.017.

Momand, J., Zambetti, G., Olson, D., George, D. and Levine, A. (1992) 'The mdm-2 oncogene product forms a complex with the p53 protein and inhi- bits p53-mediated transactivation', *Cell*, 69, pp. 1237–1245. doi: 10.1016/0092-8674(92)90644-R.

Momand J. The MDM2 gene amplification database. (1998) *Nucleic Acids Research,* 26(15), pp. 3453-3459.

Momand J, Villegas A, Belyi V. (2011) The evolution of MDM2 family genes. *Gene,* 486(1-2), pp. 23-30.

Nepple, K. G. and O'Donnell, M. A. (2009) 'The optimal management of T1 high-grade bladder cancer', *Journal of the Canadian Urological Association*, 3(6 SUPPL. 4), pp. 188–192.

Nicholson, J., Neelagandan, K., Huart, A. S., Ball, K., Molloy, M. P. and Hupp, T. (2012) 'An iTRAQ Proteomics Screen Reveals the Effects of the MDM2 Binding Ligand Nutlin-3 on Cellular Proteostasis', *Journal of Proteome Research*, 11(11), pp. 5464–5478. doi: 10.1021/pr300698d.

Parant J, Chavez-Reyes A, Little N, Yan W, Reinke V, Jochemsen A et al. (2001) Rescue of embryonic lethality in Mdm4-null mice by loss of Trp53 suggests a nonoverlapping pathway with MDM2 to regulate p53. *Nature Genetics,* 29(1), pp. 92-95.

Pei, D., Zhang, Y. and Zheng, J. (2012). Regulation of p53: a collaboration between Mdm2 and Mdmx. *Oncotarget*, 3(3).

Perou, C. M., Sùrlie, T., Eisen, M. B., Rijn, M. Van De, Jeffrey, S. S., Rees, C. A., Pollack, J. R., Ross, D. T., Johnsen, H., Akslen, L. A., Fluge, I., Pergamenschikov, A., Williams, C., Zhu, S. X., Lùnning, P. E., Brown, P. O., Botstein, D. and Grant, S. (2000) 'Molecular Portraits Breast Cancer', *Nature,* 406, pp. 747-752.

Perry, M. (2004) Mdm2 in the response to radiation. *Mol Cancer Res*, 2(1), pp. 9-19.

Perry, M. (2009). The Regulation of the p53-mediated Stress Response by MDM2 and MDM4. *Cold Spring Harbor Perspectives in Biology*, 2(1), pp.a000968-a000968.

Phelps, D. A., Bondra, K., Seum, S., Chronowski, C., Leasure, J., Kurmasheva, R. T., Middleton, S., Wang, D., Mo, X. and Houghton, P. J. (2015) Inhibition of MDM2 by RG7388 confers hypersensitivity to X-radiation in xenograft models of childhood sarcoma', *Pediatric Blood & Cancer*, 62(8), pp. 1345–1352. doi: 10.1002/pbc.25465.Inhibition.

Ren, J., Wen, L., Gao, X., Jin, C., Xue, Y. and Yao, X. (2009) 'DOG 1.0: illustrator of protein domain structures', *Cell research*, 19, pp. 271–273. doi: 10.1038/cr.2009.6.

Riley, M. F. and Lozano, G. (2012) 'The Many Faces of MDM2 Binding Partners', *Genes & cancer*, 3(3–4), pp. 226–39. doi: 10.1177/1947601912455322.

Roth, J., Dobbelstein, M., Freedman, D. A., Shenk, T. and Levine, A. J. (1998) 'Nucleo-cytoplasmic shuttling of the hdm2 oncoprotein regulates the levels of the p53 protein via a pathway used by the human immunodeficiency virus rev protein', *EMBO Journal*, 17(2), pp. 554–564. doi: 10.1093/emboj/17.2.554.

Saadatzadeh, M., Elmi, A., Pandya, P., Bijangi-Vishehsaraei, K., Ding, J., Stamatkin, C., Cohen-Gadol, A. and Pollok, K. (2017). The Role of MDM2 in Promoting Genome Stability versus Instability. *International Journal of Molecular Sciences*, 18(10), p.2216.

Saito, Y., Fujimoto, H. and Kobayashi, J. (2013) 'Role of NBS1 in DNA damage response and its relationship with cancer development', *Translational Cancer Research*, 2(3), pp. 178–189. doi: 10.3978/j.issn.2218-676X.2013.04.05.

Saito, Y. and Komatsu, K. (2015) 'Functional Role of NBS1 in Radiation Damage Response and Translesion DNA Synthesis', *Biomolecules*, 5(3), pp. 1990–2002. doi: 10.3390/biom5031990.

Schwanhausser, B. (2011) 'Global quantification of mammalian gene expression control', *Nature*, 473, pp. 337–342. doi: 10.1038/nature10098.

Schwertman, P., Bekker-Jensen, S. and Mailand, N. (2016) 'Regulation of DNA double-strand break repair by ubiquitin and ubiquitin-like modifiers', *Nature Reiewsv Moecularl Cell Biology*, 17(6), pp. 379–394. doi: 10.1038/nrm.2016.58.

Shadfan M, Lopez-Pajares V, Yuan ZM. (2012) MDM2 and MDMX: Alone and together in regulation of p53. *Transl Cancer Res,* 1(2), pp. 88-89.

Sharp, D., Kratowicz, S., Sank, M. and George, D. (1999). Stabilization of the MDM2 Oncoprotein by Interaction with the Structurally Related MDMX Protein. *Journal of Biological Chemistry*, 274(53), pp.38189-38196.

Shi, D. and Gu, W. (2012) 'Dual Roles of MDM2 in the Regulation of p53: Ubiquitylation Dependent and Ubiquitylation Independent Mechanisms of MDM2 Repression of p53 Activity', *Genes & cancer*, 3(3–4), pp. 240–8. doi: 10.1177/1947601912455199.

Shiloh Y. (2006) The ATM-mediated DNA-damage response: taking shape. *Trends in Biochemical Sciences,* 31(7), pp. 402-410.

Simon R, Struckmann K, Schraml P, Wagner U, Forster T, Moch H et al. (2002) Amplification pattern of 12q13-q15 genes (MDM2, CDK4, GLI) in urinary bladder cancer. *Oncogene,* 21(16), pp. 2476-2483.

Sjödahl, G., Lauss, M., Lövgren, K., Chebil, G., Gudjonsson, S., Veerla, S., Patschan, O., Aine, M., Fernö, M., Ringnér, M., Månsson, W., Liedberg, F., Lindgren, D. and Höglund, M. (2012) 'A molecular taxonomy for urothelial carcinoma', *Clinical Cancer Research*, 18(12), pp. 3377–3386. doi: 10.1158/1078-0432.CCR-12-0077-T.

Stefanou DG, Nonni AV, Agnantis NJ, Athanassiadou SE, Briassoulis E, Pavlidis N. (1998) p53/MDM-2 immunohistochemical expression correlated with proliferative activity in different subtypes of human sarcomas: a ten-year follow-up study. *Anticancer Res*, 18(6B), pp. 4673-4681.

Strano, S., Dell'Orso, S., Di Agostino, S., Fontemaggi, G., Sacchi, A. and Blandino, G. (2007) 'Mutant p53: an oncogenic transcription factor', *Oncogene*, 26(15), pp. 2212–2219. doi: 10.1038/sj.onc.1210296.

Supiot, S., Hill, R. P. and Bristow, R. G. (2008) 'Nutlin-3 radiosensitizes hypoxic prostate cancer cells independent of p53', *Molecular cancer therapeutics*, 7(4), pp. 993–999. doi: 10.1158/1535-7163.MCT-07-0442.

Takada, K., Nasu, H., Hibi, N., Tsukada, Y., Shibasaki, T., Fujise, K., Fujimuro, M., Sawada, H., Yokosawa, H. and Ohkawa, K. (1997) 'Serum concentrations of free ubiquitin and multiubiquitin chains', *Clinical Chemistry*, 43(7), pp. 1188–1195.

Tang, Y., Zhao, W., Chen, Y., Zhao, Y. and Gu, W. (2008). Acetylation Is Indispensable for p53 Activation. *Cell*, 133(4), pp.612-626.

The Cancer Genome Atlas Research Network (2014) 'Comprehensive molecular characterization

of urothelial bladder carcinoma.', *Nature*, 507(7492), pp. 315–22. doi: 10.1038/nature12965.

Tian, Q., Serguei, S., Mao, M., Weng, L., Feetham, M. C., Doyle, M. J., Yi, E. C., Dai, H., Thorsson, V., Eng, J., Goodlett, D., Berger, J. P., Gunter, B., Linseley, P. S., Stoughton, R. B., Aebersold, R., Collins, S. J., Hanlon, W. A. and Hood, L. E. (2004) 'Integrated Genomic and Proteomic Analyses of Gene Expression in Mammalian Cells', *Molecular & Cellular Proteomics*, 3(10), pp. 960–969. doi: 10.1074/mcp.M400055-MCP200.

Toledo F, Wahl G. Regulating the p53 pathway: in vitro hypotheses, in vivo veritas. (2006) *Nature Reviews Cancer,* 6(12), pp. 909-923.

Tonsing-Carter, E., Bailey, B. B., Reza, S. M., Ding, J., Wang, H., Sinn, A. L., Peterman, K. M., Spragins, T. K., Silver, J. M., Sprouse, A. A., Georgiadis, T. M., Gunter, T. Z., Long, E. C., Hanenberg, R., Territo, P. R., Sandusky, G. E., Mayo, L. D., Eischen, C. M., Shannon, H. E. and Pollok, K. E. (2015) 'Potentiation of carboplatin-mediated DNA damage by the Mdm2 modulator Nutlin-3a in a humanized orthotopic breast-to-lung metastatic model', *Molecular Cancer Therapeutics*, 14(12), pp. 2850–2863. doi: 10.1002/dev.21214.

Tsai, W., Wang, Z., Yiu, T. T., Akdemir, K. C., Xia, W., Winter, S., Tsai, C., Shi, X., Schwarzer, D., Plunkett, W., Aronow, B., Gozani, O., Fischle, W., Hung, M., Patel, D. J. and Barton, M. C. (2010) 'TRIM24 links a noncanonical histone signature to breast cancer', *Nature,* 468(7326), pp. 927–932. doi:10.1038/nature09542.

Uchida T, Minei S, Gao J, Wang C, Satoh T, Baba S. (2002) Clinical significance of p53, MDM2 and bcl-2 expression in transitional cell carcinoma of the bladder. *Oncology Reports,* 9(2), pp. 253-259.

Uziel T. (2003) Requirement of the MRN complex for ATM activation by DNA damage. *The EMBO Journal,* 22(20), pp. 5612-5621.

Valentine, J. M., Kumar, S. and Moumen, A. (2011) 'A p53-independent role for the MDM2 antagonist Nutlin-3 in DNA damage response initiation', *BMC cancer*, 11(1), p. 79. doi: 10.1186/1471-2407-11-79.

Van Batavia, J., Yamany, T., Molotkov, A., Dan, H., Mansukhani, M., Batourina, E., Schneider, K., Oyon, D., Dunlop, M., Wu, X., Cordon-Cardo, C. and Mendelsohn, C. (2014). Bladder cancers arise from distinct urothelial sub-populations. *Nature Cell Biology*, 16(10), pp.982-991.

Varon R, Vissinga C, Platzer M, Cerosaletti K, Chrzanowska K, Saar K et al. (1998) Nibrin, a Novel DNA Double-Strand Break Repair Protein, Is Mutated in Nijmegen Breakage Syndrome. *Cell*, 93(3), pp. 467-476.

Villalonga-Planells, R., Coll-Mulet, L., Martinez-Soler, F., Castano, E., Acebes, J. J., Gimenez-Bonafe, P., Gil, J. and Tortosa, A. (2011) 'Activation of p53 by nutlin-3a induces apoptosis and cellular senescence in human glioblastoma multiforme', *PLoS ONE*, 6(4). doi: 10.1371/journal.pone.0018588.

Vogel, C., Abreu, R. de S., Ko, D., Le, S.-Y. Y., Shapiro, B. A., Burns, S. C., Sandhu, D., Boutz, D. R., Marcotte, E. M. and Penalva, L. O. (2010) 'Sequence signatures and mRNA concentration can explain two-thirds of protein abundance variation in a human cell line. TL - 6', *Molecular systems biology*, 6 (400), p. 400. doi: 10.1038/msb.2010.59.

Wang, P., Lushnikova, T., Odvody, J., Greiner, T. C., Jones, S. N. and Eischen, C. M. (2008) 'Elevated

Mdm2 expression induces chromosomal instability and confers a survival and growth advantage to B cells', *Oncogene*, 27(11), pp. 1590–8. doi: 10.1038/sj.onc.1210788.

Wawrzynow, B., Zylicz, A., Wallace, M., Hupp, T. and Zylicz, M. (2007) 'MDM2 chaperones the p53 tumor suppressor', *Journal of Biological Chemistry*, 282(45), pp. 32603–32612. doi: 10.1074/jbc.M702767200.

Way, L., Faktor, J., Dvorakova, P., Nicholson, J., Vojtesek, B., Graham, D., Ball, K. L. and Hupp, T. (2016) 'Rearrangement of mitochondrial pyruvate dehydrogenase subunit dihydrolipoamide dehydrogenase protein-protein interactions by the MDM2 ligand nutlin-3', *Proteomics*, 16(17), pp. 2327–2344. doi: 10.1002/pmic.201500501.

Wei Dai Y. (2014) Genomic Instability and Cancer. *Journal of Carcinogenesis & Mutagenesis,* 05(02).

Williams, S. V., Adams, J., Coulter, J., Summersgill, B. M., Shipley, J. and Knowles, M. A. (2005) 'Assessment by M-FISH of karyotypic complexity and cytogenetic evolution in bladder cancer in vitro', *Genes Chromosomes and Cancer*, 43(4), pp. 315–328. doi: 10.1002/gcc.20166.

Wu, J., Zhang, X., Zhang, L., Wu, C., Rezaeian, A. H., Chan, C., Li, J., Wang, J., Gao, Y., Han, F., Jeong, Y. S., Yuan, X., Khanna, K. K., Jin, J., Zeng, Y. and Lin, H. (2012) 'Skp2 E3 Ligase Integrates ATM Activation and Homologous Recombination Repair by Ubiquitinating NBS1', *Molecular Cell*, 46(3), pp. 351–361. doi: 10.1016/j.molcel.2012.02.018.

Xirodimas, D., Saville, M., Bourdon, J., Hay, R. and Lane, D. (2004). Mdm2-Mediated NEDD8 Conjugation of p53 Inhibits Its Transcriptional Activity. *Cell*, 118(1), pp.83-97.

Yu Q, Li Y, Mu K, Li Z, Meng Q, Wu X et al. (2014) Amplification of Mdmx and overexpression of MDM2 contribute to mammary carcinogenesis by substituting for p53 mutations. *Diagnostic Pathology*, 9(1), pp. 71.

Zhang R, Wang H. (2000) MDM2 Oncogene as a Novel Target for Human Cancer Therapy. *Current Pharmaceutical Design,* 6(4), pp. 393-416.

Zietz C, Rössle M, Haas C, Sendelhofert A, Hirschmann A, Stürzl M et al. MDM-2 Oncoprotein Overexpression, p53 Gene Mutation, and VEGF Up-Regulation in Angiosarcomas. (1998) The *American Journal of Pathology,* 153(5), pp. 1425-1433.

Appendix 1

Copy number variation analysis in eight bladder cancer and one normal human urothelial cell lines using Nexus Copy Number software.

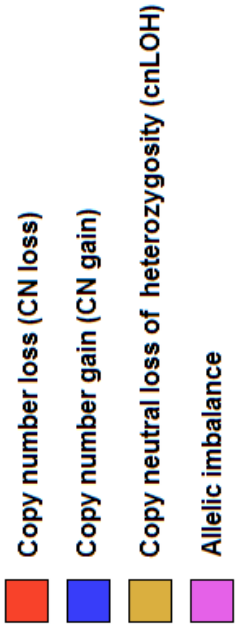

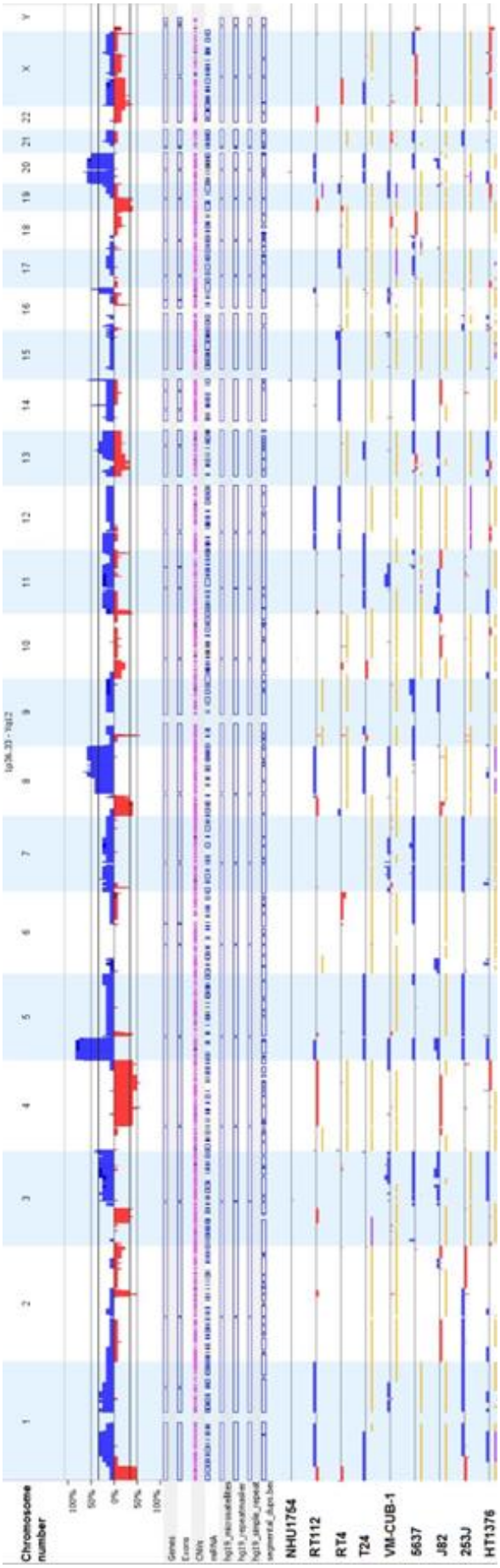

Appendix 2

Combined results of CNV and mutation status of MDMD2 and NBS1 in 11 studies (1889 patients/1934 samples) available via the cBioPortal for Cancer Genomics (http://www.cbioportal.org/) (Guo *et al.,* 2013).